Thrust Surface Method: An innovative approach for the three-dimensional lower bound Limit Analysis of masonry vaults

Thrust Surface Method: an innovative approach for the three-dimensional lower bound Limit Analysis of masonry vaults

Aguinaldo Fraddosio [a], *Nicola Lepore** [a], *Mario Daniele Piccioni* [a]

[a] *Department of Civil Engineering Sciences and Architecture, Polytechnic University of Bari, Italy.*

E-mail addresses: aguinaldo.fraddosio@poliba.it (A. Fraddosio), nicola.lepore@poliba.it (N. Lepore), mariodaniele.piccioni@poliba.it (M.D. Piccioni).

ORCiDs: http://orcid.org/0000-0001-6185-1202 (A. Fraddosio), https://orcid.org/0000-0001-9475-3772 (M.D. Piccioni).

**Corresponding author. Polytechnic University of Bari, via Re David, 70125 Bari, Italy.*

Abstract

We propose a new computational equilibrium approach for the structural safety assessment of historical masonry vaults of any geometry under general loading conditions. This approach, called Thrust Surface Method (TSM), represents an innovative application of the lower bound theorem of Limit Analysis to masonry vaults modeled as continuous No-Tension bodies. In particular, on allowing for singular stresses, the search of statically admissible stress field is reduced to the search of purely compressed membranes in equilibrium with the applied loads and entirely contained into the thickness of the vault. Based on a convenient numerical procedure and the formulation of a suitable constrained optimization problem, TSM is a method of practical application that, looking for "extremal" or "optimal" solutions, is capable of fully exploring the entire load-bearing capacity spectrum of a vault having an arbitrary geometry. Since the particular formulation, TSM can take into account not only any kind of vertical loads, but also horizontal loads like those simulating the maxima inertia effects related to seismic actions. In addition, the proposed approach could be a useful tool for visualizing and understanding the complex three-dimensional behavior and the close relationship between form and structure characterizing masonry vaults.

The effectiveness and the capabilities of the method are discussed in light of some representative case studies, allowing for suitable comparisons with the results of other analytical and experimental approaches in the literature.

Keywords: *historic constructions; masonry vaults; limit analysis; equilibrium; numerical methods; lower bound theorem; thrust surface.*

1. Introduction

Masonry structures are the vast majority of the worldwide Architectural Heritage, which needs to be preserved for future generations. Despite the great interest of the scientific community and the large number of research works on the subject [1,2], there is still the need of research toward the formulation of widely accepted structural analysis approaches for historical masonry constructions, especially if structures with complex geometry as vaults and domes are considered.

Indeed, it is well-known that linear elastic analysis is inadequate for understanding the structural behavior of masonry structures [3]. Indeed, in Literature it is possible to find advanced mechanical models, that consider issues like anisotropy, nonlinear material behavior, plasticity, and damage, for describing the complex behavior of masonry structures. But the employ of the above models may be obstructed in several applicative cases by the difficulty in performing the accurate and extensive mechanical tests and surveys needed for the characterization of the high number of mechanical parameters of the masonry and of the boundary condition. Inaccuracy in the materials characterization or in the boundary condition characterization may yield results very far from the actual structural behavior of the construction. This is generally the case of historical masonry structures, where material parameters describing strength and stiffness are generally affected by a large heterogeneity and by a high level of uncertainty.

Nowadays, considering the difficulties in an accurate and representative structural modeling of masonry, an increasing number of researchers consider convenient to renounce to describe the load-response behavior, focalizing only on the estimation of the collapse loads. This approach, which can be set in the theoretical framework of Limit Analysis, is actually getting a growing consensus in the literature [4–8].

Indeed, from the theoretical point of view we recall that in most cases, since masonry usually has a very small tensile strength, the only reasonable assumption that it is possible to make is that the material behaves unilaterally, i.e. the masonry has no tensile strength at all (No-Tension models). A complete mathematical formalization of No-Tension material models is mainly attributable to the Italian School of Structural Mechanics [9–13]. Furthermore, Del Piero in [14] proved that Limit Analysis theorems apply also for No-Tension materials.

In this vein, one of the milestones toward the understanding of the mechanics of historical masonry structures is due to Heyman [15,16], who wisely reread the “geometrical” and “equilibrium-based” theories used by the ancient master builders within the rational framework of the modern Limit Analysis. It is worth to point out that, despite the very different starting points and methodologies, both old (ancient master builders’ knowledge) and new (Limit Analysis for No-Tension materials) theories come to the same conclusion: the safety of a masonry structure is a matter of geometry, and then a safe state of equilibrium can be achieved only through a suitable geometry. As evidence of this, it is well-known that by the lower bound theorem of Limit Analysis for No-Tension materials a masonry arch is “safe” under given loads if it is possible to find an equilibrium thrust line entirely contained into the thickness of the arch.

This equilibrium approach, used since the antiquity (although in an unwitting way) for the stability assessment of masonry structures reducible to plane schemes, like arches, can be extended also to spatial structures as domes and vaults using the classical slicing technique, consisting in the decomposition of the three-dimensional structure in a series of plane schemes (slices of the actual structure). Nevertheless, this approach, described in detail in [17], neglects any possible three-dimensional feature of the structural behavior: thus, according to the lower bound theorem of Limit Analysis, if any a statically admissible solution it is found by the slicing technique, this solution strongly underestimates the actual load-bearing capacity of the vault.

Recent studies on the subject have tried to overcome this drawback, proposing both kinematic and static Limit Analysis approaches able to take into account the complex three-dimensional structural behavior of masonry vaults, and thus to give a substantially better load-bearing capacity estimate. These studies are progressively gaining a growing consensus, although some criticisms regarding the generality of the classic static Limit Analysis approaches still remain. In particular, criticisms concern the role of the frictional sliding in the collapse of masonry structures [18–20], that is neglected by classic Limit Analysis theory. Anyway, for masonry vaults and domes the assumption of no frictional sliding may yield representative results in terms of load bearing capacity for most of the practical applications with indisputable advantages in simplifying analytical aspect. This holds especially for historical vaults, where the joints between blocks are suitably arranged through an accurate and wise stereotomic design.

In this context, among the kinematic Limit Analysis approaches we recall that proposed by Milani et al. in [21] and based on a six-node triangular curved element, where an upper bound of the collapse load is obtained admitting plastic dissipation only at the interfaces between adjoining elements. Moreover, in [22,23], a Genetic Algorithm-NURBS-based approach for the kinematic limit analysis of FRP-reinforced masonry vaults is developed.

On the other hand, from the static point of view, O'Dwyer [24] and Block et al. [25,26] proposed lower bound Limit Analysis approaches based on discrete networks that configure the search of a statically admissible stress field as the search of a purely compressed spatial network in equilibrium with the applied loads and entirely contained within the thickness of the masonry vault; some applicative issues are discussed in [27,28]. Recently, further developments of these approaches are proposed in [29,30]. Anyhow, the quality of solutions depends on the chosen discretization of the problem, i.e., on the topology of the network that has to be a priori chosen [31].

Also continuum approaches for lower bound Limit Analysis of masonry vaults and domes were recently proposed [32–34]. In particular Angelillo et al., allowing for singular stress fields according to the theory for No-Tension 2D bodies equilibrium introduced by Lucchesi et al. in [35–37], developed an analytical method configuring the search of statically admissible stress fields for masonry vaults as the search of unilateral membranes in equilibrium with the applied loads and entirely contained into the thickness of the vault [38–40]. The geometry of these membranes is described *a la Monge* while their equilibrium is formulated adopting the Pucher form [41] and solved by introducing the Airy stress function. In this way, the problem is formulated in terms of a partial differential equation in two unknown scalar functions: the Airy stress function F and the shape function of the membrane f. The approach by Angelillo et al. is characterized by an advanced and rigorous formulation of the equilibrium problem, and has the merit of clearly highlighting the close relationship between form and structure that is a hallmark of masonry curved structures. Possible strategies for solving the equilibrium problem above described are suggested in [38]: for the simple case of uniform vertical loads on the horizontal projection of the vaults and for some special vault geometries, closed-form solutions can be found by following mainly two approaches: a) assigning a priori the geometry of a membrane f entirely contained into the thickness of the vault and determining the stress function F by solving the equilibrium differential equation; in this case, it is necessary to a posteriori verify if the obtained stress field related to F is actually statically admissible; b) starting from an apriori assigned class of statically admissible stress fields represented by a stress function F, determine the shape function f by solving of the equilibrium differential equation; now, it is necessary to a posteriori verify if the obtained membrane f is actually contained in the thickness of the vault. In [38] it is also proposed an iterative procedure that combines the two above described approaches.

The need for a priori assumptions, on one hand, allows for finding closed-form solutions for some applicative cases, but on the other hand, prevents from considering more complex geometries and/or loading conditions; furthermore, if a solution is determined it is possible to claim that the vault can withstand the assigned loads, but it is not possible to assess how far is this solution from the actual maximum load-bearing capacity of the structure. Moreover, a priori assumptions prevent from determining extremal solutions like those related to the maximum or the minimum thrust on the abutments, or the maximum level of variable loads bearable by the structure. Finally, it became very difficult to take into account also horizontal loads; by the way, it is in these cases that the issues above listed are more relevant.

In order to overcome the limitations just mentioned, in this paper we propose a numerical method for the lower bound Limit Analysis of masonry vaults and domes called the Thrust Surface Method (TSM). TSM is developed in the theoretical framework of the continuum approach by Angelillo et al. that is capable of determining at the same time the two unknown functions of the problem, the Airy stress function F and the shape function of the membrane f, and of tackling problems of vaults having any shape and under the action of arbitrary loading conditions. This goal is achieved by a convenient numerical formulation and by configuring the problem as a suitable constrained optimization problem, by following an approach similar of that proposed by some of the authors in [42] for searching optimal lower bound solutions in the very different context of non-linear elastic problems. No a priori assumptions on the unknown functions are needed, nor on the load paths or on the topology of the network, as in the discrete equilibrium approaches cited above. This way, TSM reveals to be able of significantly extending the capability of the equilibrium approach in [38–40] in terms of possible geometries and loading conditions that can be studied, and of improving definitely the quality of the obtainable solutions, providing the possibility of a comprehensive exploration of the whole set of statically admissible solutions. Indeed, TSM avoids any a priori choice on the functions F or f and allows for the determination of "extremal" or "optimal" solutions, and then of of exploring the whole load-bearing capacity spectrum of the structure, and not only of determining "just one" safe solution. The formulation of the method allows for analyzing vaults whose shape is defined not only by arbitrary analytic functions, but also by a cloud of points, as supplied for example by a laser scanner survey.

Moreover, in addition to any kind of vertical loads (starting from the self-weight, to more complex loading conditions, like for example those due to the infill) also horizontal loads can be taken into account. The latter could represent the maxima inertia effects due to seismic actions, and therefore TSM can also answer to the crucial question of evaluating the seismic load bearing capacity of masonry vaults and domes [43].

In our opinion, TSM represents an approach for the structural analysis of masonry vaults and domes very close to the needs emerging in practical applications and might be easily implemented in software tools to be employed by practitioners. One of the most interesting features of TSM in view of practical applications is just the capability of determining "optimal" lower bound solutions, that allows for facing several relevant problems. For example, in some applications the structure cannot withstand safely the assigned loads, i.e., it is impossible to find a statically admissible solution. In these cases, it is important to determine, especially for what concerns eventual variable loads like seismic loads, the portion of the assigned loads compatible with the structural safety of the construction. This study requires a method for approximating as closely as possible the actual structural capacity and aims at limit strengthening interventions to those strictly needed, as it is proper for historical and monumental constructions. Moreover, when dealing with constructions having complex geometries like vaults and domes likely heuristic procedures for constructing "a" statically admissible solution not allow for identifying a safe solution under the assigned loads, whereas such a solution exists: approaches based on an optimization procedure may overcome this limitation. Finally, the capability of optimal lower bound solutions allows TSM also to give a satisfactory answer to the search of the maximum or the minimum thrust on the abutments.

This paper is essentially devoted to the formulation of the Thrust Surface Method (TSM) approach. We describe in detail the features of TSM and then we validate the proposed innovative approach with reference to some case studies regarding masonry vaults under the action of the self-weight. Indeed, the latter simple load condition allows us for comparing the results obtained by TSM with some well-established analytical and numerical results in the literature. In forthcoming papers, we will discuss the capability of TSM also for problems characterized by more complex geometries and/or load conditions.

The paper is organized as follows.

In *Sect. 2* we recap some fundamental theoretical concept about equilibrium analysis of masonry vaults. In particular, in *Sect. 2.1* the Rigid No-Tension Material model (RNT) is summarized, along with the lower bound theorem of Limit Analysis for masonry structures; the strategy of using singular stress fields for solving the equilibrium problem is also recalled. In *Sect. 2.2* the main features of the equilibrium Limit Analysis approach proposed for masonry vaults and domes in [38–40] are reported.

In *Sect. 3* the TSM method is stated. In particular, *Sect. 3.1* concerns the assignation of the input data (geometry and loading conditions) and of the constraints for the constrained optimization problem, coming from the equilibrium and the unilaterality requirements. In *Sect. 3.2* the assignment of boundary conditions and other constraints is described; among the latter, the constraint capable of taking into account the influence on the solution of preexisting cracks. *Sect. 3.3* regards the possible objective functions, aimed at determining the Geometrical Factor of Safety of the vault, maximum and minimum thrust solutions and a lower bound estimation of collapse loads in an increasing loading process. In *Sect. 3.4* the fundamental concepts for the numerical approximation of the solution are introduced. Finally, in *Sect. 3.5* the algorithms employed for the optimization are summarized.

In *Section 4* we describe the main steps of TSM approach.

In *Section 5* the effectiveness and the capabilities of TSM are discussed in light of some representative case studies, also by suitable comparison with the results of other analytical and experimental approaches in the literature. In particular, in *Sect. 5.1* the load assignation valid for all the examined case studies is described; an expression of vertical loads describing more accurately the self-weight, whose projection on the horizontal plane is not constant, is given. The first case study is analyzed in *Sect. 5.2*: a barrel vault; this case is considered since the simplicity of the geometry makes it useful for the validation of the results. The more complex case of a cross vault is then studied in *Sect. 5.3*.

2. The equilibrium of masonry vaults

2.1 The Rigid No-Tension model (RNT) and singular stress fields

We consider a generic vault represented by $\mathscr{B} \in \mathbb{R}^3$, in equilibrium with the applied loads (**s**,**b**), with **s** tractions on the unconstrained part of the boundary $\partial\mathscr{B}^s$ and **b** the body forces; let the complementary constrained part of the boundary $\partial\mathscr{B}^r := \partial\mathscr{B} \backslash \partial\mathscr{B}^s$ be fixed. Moreover, we assume that the displacement **u** and the related strain **E** are infinitesimal.

If the vault is composed by a continuous Rigid No-Tension Material (RNT), the stress tensor **T** have to be negative semidefinite,

$$\mathbf{T} \in Sym^{-}; \tag{2}$$

in addition, since there are no elastic strains, the infinitesimal strain tensor **E** corresponds to inelastic strains related to fractures into the material (both concentrated and smeared fractures), and it has to be positive semidefinite:

$$\mathbf{E} \in Sym^{+}. \tag{3}$$

Moreover, we assume that the (Cauchy) stress **T** does not work for the corresponding strain **E**:

$$\mathbf{T} \cdot \mathbf{E} = 0. \tag{4}$$

According to [14], these constitutive assumptions generalize the classical Heyman's assumptions. Indeed, they correspond to the requirement for **E** to be normal to the cone of admissible stresses $\mathbf{T} \in Sym^{-}$ and allow for the application of the two theorems of Limit Analysis.

In view of the lower bound theorem of Limit Analysis, it is of interest the search for $\mathscr{B}$ of statically admissible stress fields, in equilibrium with assigned loads and such that $\mathbf{T} \in Sym^{-}$. To this aim, by following [36] and [44,45], for RNT material it is possible to admit stresses $\mathbf{T}$ that are only summable distributions i.e.:

$$\int_{\mathscr{B}} \|\mathbf{T}\| < \infty, \tag{5}$$

which, in general, can be decomposed into the sum

$$\mathbf{T} = \mathbf{T}_{\mathbf{r}} + \mathbf{T}_{\mathbf{s}} \tag{6}$$

of a regular part $\mathbf{T}_{\mathbf{r}}$, and a singular part $\mathbf{T}_{s}$.

In this hypothesis, we can assume that $\mathbf{T}$ is balanced and singular across a surface $\mathscr{S}$ contained inside the vault $\mathscr{B}$; this corresponds to assume that $\mathbf{T}$ is a surface Dirac delta over $\mathscr{S}$. Indeed, by using a classical criterion of static equivalence, the forces (**b**, **s**) applied to the vault $\mathscr{B}$ can be reduced to a system of tractions **p** applied at the extrados of the vault [38].

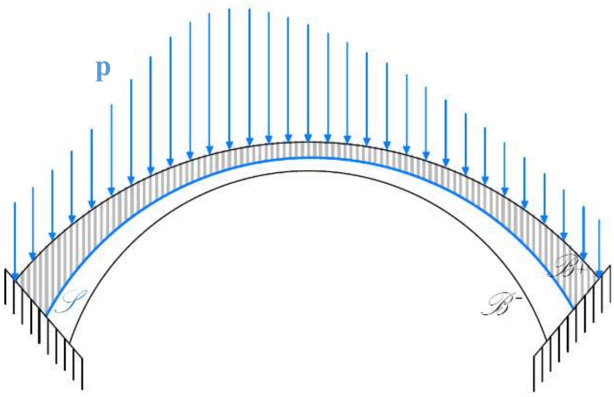

Figure 1. Scheme of a generic cross section of a vault [38]

Now, by following the approach in [38], we consider a surface $\mathscr{S}$ entirely contained in $\mathscr{B}$ and dividing the vault into two parts: $\mathscr{B}^{+}$ (above $\mathscr{S}$) and $\mathscr{B}^{-}$ (below $\mathscr{S}$), where $\mathscr{B}^{+}$ is in a state of uniaxial compression and $\mathscr{B}^{-}$ is inert (zero stress) (Figure 1). In these assumptions, and for the equilibrium, the surface $\mathscr{S}$ is loaded by the stress jump across $\mathscr{S}$ between $\mathscr{B}^{+}$ and $\mathscr{B}^{-}$. Furthermore, for the admissibility of the stress (2) the generalized membrane stresses $\mathbf{S}$ on the surface $\mathscr{S}$ must be a negative semidefinite tensor.

Therefore, the search of statically admissible stress fields for the vault $\mathscr{B}$ is reduced to the search of a unilateral membrane $\mathscr{S}$ entirely contained into the thickness of the vault and in equilibrium with the assigned loads. For more detail about the use of singular stress fields for masonry-like structure, the interested reader can refer to [44].

2.2 The equilibrium of unilateral membrane

In a Cartesian reference system $O(x,y,z)$, let's consider a membrane $\mathscr{S}$ that can be described using the *Monge* patch[1] as follows:

$$z = f(x,y), \quad (x,y) \in \Psi, \tag{7}$$

where Ψ is the projection of the vault on the plane (x,y). The equilibrium of such membrane $\mathscr{S}$ under the load $\mathbf{p}(p_x, p_y, p_z)$ can be expressed in the Pucher form [41].

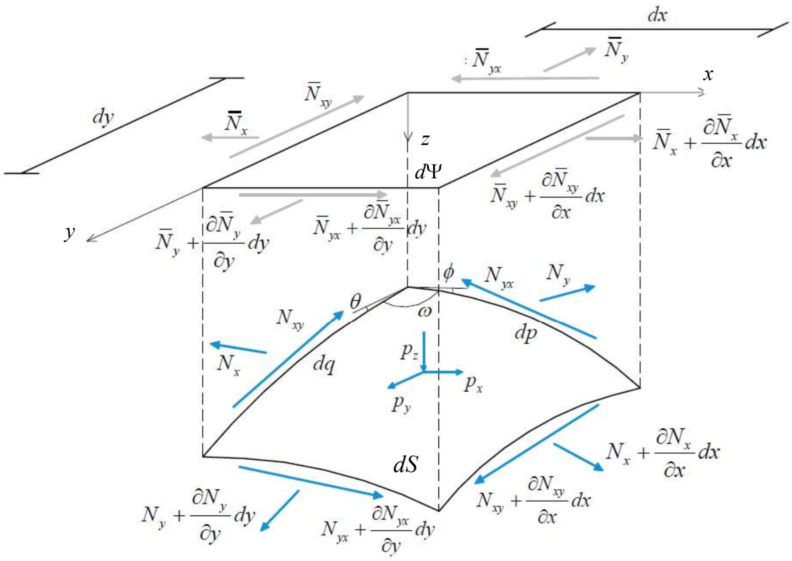

Figure 2. Equilibrium of an infinitesimal element of the membrane dS; the edges *dp* and *dq* project in the (*x*,*y*) plane into *dx* and *dy*, respectively.

In particular, with reference to Figure 2, if we consider the projections $\bar{N}_x, \bar{N}_y, \bar{N}_{xy}$ of the membrane stresses N_x, N_y, N_{xy} on Ψ, we have:

$$\bar{N}_x = N_x \frac{\cos\phi}{\cos\theta}; \quad \bar{N}_y = N_y \frac{\cos\theta}{\cos\phi}; \quad \bar{N}_{xy} = N_{xy}, \tag{8}$$

where ϕ and θ are the angles formed by the membrane edges with the axes *x* and *y*, respectively, and:

$$\cos\phi = 1 \Big/ \sqrt{1 + \left(\frac{\partial f}{\partial x}\right)^2}; \quad \cos\theta = 1 \Big/ \sqrt{1 + \left(\frac{\partial f}{\partial y}\right)^2}. \tag{9}$$

The equilibrium in *x*-direction and *y*-direction yields:

[1] The Monge patch is a most straightforward parametrization in which a surface is defined by giving its height *z* over some plane as a function of orthonormal coordinates *x* and *y* in the plane. Notice that, from the definition, a Monge patch could not be able to entirely describe a surface of a vault unless introducing suitable differentiable manifolds. However, the above-mentioned case is very rare and this kind of parametrization is acceptable for the greatest part of the applicative cases.

$$\begin{cases} \dfrac{\partial \bar{N}_x}{\partial x} + \dfrac{\partial \bar{N}_{yx}}{\partial y} + \bar{p}_x = 0 \\ \dfrac{\partial \bar{N}_y}{\partial y} + \dfrac{\partial \bar{N}_{xy}}{\partial x} + \bar{p}_y = 0, \end{cases} \tag{10}$$

respectively, while for the equilibrium in the z-direction it is:

$$\bar{N}_x \frac{\partial^2 f}{\partial x^2} + \bar{N}_y \frac{\partial^2 f}{\partial y^2} + 2\bar{N}_{xy} \frac{\partial^2 f}{\partial x \partial y} = -\bar{p}_z + \bar{p}_x \frac{\partial f}{\partial x} + \bar{p}_y \frac{\partial f}{\partial y}, \tag{11}$$

where $\left(\bar{p}_x, \bar{p}_y, \bar{p}_z\right)$ are the loads for unit area of the projection Ψ equivalent to $\left(p_x, p_y, p_z\right)$, that is:

$$\bar{p}_x = p_x \psi\left(\phi,\theta\right); \quad \bar{p}_y = p_y \psi\left(\phi,\theta\right); \quad \bar{p}_z = p_z \psi\left(\phi,\theta\right), \tag{12}$$

with

$$\psi\left(\phi,\theta\right) = \frac{\sqrt{1-\sin^2\phi \sin^2\theta}}{\cos\phi\cos\theta} \tag{13}$$

the ratio between the area of the infinitesimal membrane element dS and the area of its horizontal projection $dxdy$ (Figure 2) [41].

Solutions for the system of the three equilibrium equations (10)-(11) can be obtained introducing an Airy stress function $F\left(x,y\right)$ such that [41]:

$$\bar{N}_x = \frac{\partial^2 F}{\partial y^2} - \int \bar{p}_x \, dx; \quad \bar{N}_y = \frac{\partial^2 F}{\partial x^2} - \int \bar{p}_y \, dy; \quad \bar{N}_{xy} = -\frac{\partial^2 F}{\partial x \partial y}, \tag{14}$$

that identically verify the two equilibrium equations (10). Substituting (14) in (11) we get:

$$\frac{\partial^2 F}{\partial x^2}\frac{\partial^2 f}{\partial y^2} - 2\frac{\partial^2 F}{\partial x \partial y}\frac{\partial^2 f}{\partial x \partial y} + \frac{\partial^2 F}{\partial y^2}\frac{\partial^2 f}{\partial x^2} = q, \tag{15}$$

where q collects all the load components:

$$q = -\bar{p}_z + \bar{p}_x \frac{\partial f}{\partial x} + \bar{p}_y \frac{\partial f}{\partial y} + \frac{\partial^2 f}{\partial x^2}\int \bar{p}_x \, dx + \frac{\partial^2 f}{\partial y^2}\int \bar{p}_y \, dy. \tag{16}$$

In conclusion, the equilibrium of a generic-shaped membrane is reduced to the sole (15), a second-order PDE in two unknown functions: f (describing the shape of the membrane) and F (the Airy stress function). Moreover, the requirement of negative semidefiniteness for the stress tensor **T** yields the following condition on the membrane stress tensor **S**:

$$tr\mathbf{S} \le 0 \;\; \& \;\; \det\mathbf{S} \ge 0. \tag{17}$$

Notice that, if only vertical loads are acting on the vault, the expression (16) is greatly simplified and (17) is equivalent to the requirement that the stress function *F* must be concave [12,44], that is:

$$\frac{\partial^2 F}{\partial x^2}+\frac{\partial^2 F}{\partial y^2}\leq 0 \quad \& \quad \frac{\partial^2 F}{\partial x^2}\frac{\partial^2 F}{\partial y^2}-\left(\frac{\partial^2 F}{\partial x \partial y}\right)^2 \geq 0. \tag{18}$$

3. Thrust Surface Method: searching for a statically admissible stress field as an optimization process

In this Section, we formulate the Thrust Surface Method (TSM), a new numerical method for solving the equilibrium problem presented in *Sect. 2.* TSM gives as the solution both the unknown functions *f* and *F*, and this it is capable to simultaneously determine the geometry of the membrane *f* and the Airy stress function *F* for masonry vaults of any geometry and under general load conditions, also including horizontal loads representative of seismic actions [46,47].

To this aim, if the geometry of the vault and the loads are known, a constrained optimization problem can be formulated in the form:

$$\begin{array}{lll} \min | \max & \zeta\left(x_1,\ldots,x_i\right) & i=1,\ldots,n \\ \text{subject to} & g_j\left(x_1,\ldots,x_i\right)=c_j & j=1,\ldots,m \\ & h_k\left(x_1,\ldots,x_i\right)\geq d_k & k=1,\ldots,l, \end{array} \tag{19}$$

where a suitable *n*-variables objective function $\zeta\left(x_1,\ldots,x_i\right)$ has to be maximized or minimized under *m* equality constraints $g_j\left(x_1,\ldots,x_i\right)=c_j$ and *l* inequality constraints $h_k\left(x_1,\ldots,x_i\right)\geq d_k$.

3.1 Input data and constraints of the optimization process

Since for vaults with arbitrary geometries and loading conditions it is practically impossible to obtain closed-form solutions, and since by within RNT constitutive model the equilibrium problem for masonry vaults is essentially brought back to a geometric problem, it is possible to build up strategies for searching numerical solutions inspired by typical methods of differential geometry, also used in other fields of applied mathematics and computer graphics [48–50].

In particular, it is possible to discretize the problem of the search of statically admissible stress fields through the introduction of an appropriate set of points $\mathscr{P}$, like for example a *n x m* grid of points on the horizontal projection Ψ of the vault (Figure 3a):

$$\mathscr{P} := \left\{ \mathrm{P}_{ij}\left(x_i, y_j\right) \in \Psi \right\}_{i=0,j=0}^{n,m}. \tag{20}$$

For each point, input data related to the geometry of the vault and to the load condition will be associated.

Defining *a la Monge* the functions describing the geometry of the vault $f_{int}(x,y)$, $f_{ext}(x,y)$, $f_m(x,y)$, (intrados, extrados and middle surface functions, respectively) and expressing the load condition q per unit of area of the horizontal projection Ψ, for each point $P_{ij} \in \mathscr{P}$ it is possible to associate the height of the intrados, of the extrados, of the middle surface and of the value of the load (Figure 3b).

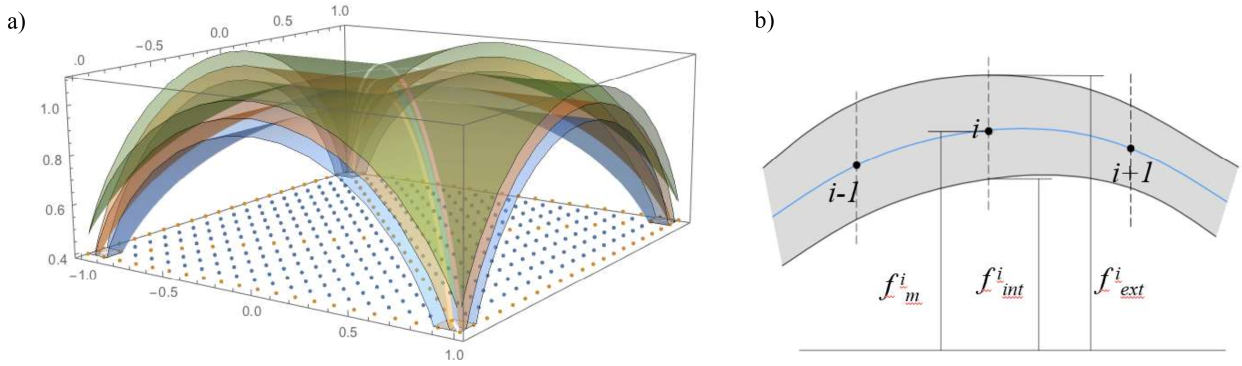

Figure 3. (a) Intrados, extrados and middle surfaces of the vault (in blue, green and orange, respectively); (b) Input data associated to each point P_{ij} of $\mathscr{P}$.

Remark: since the geometry is assigned as the height of the intrados, of the extrados, and of the middle surface in a set of discrete points, TSM can be applied not only to vault whose geometry is defined by analytic expression of the functions $f_{int}(x,y)$, $f_{ext}(x,y)$, $f_m(x,y)$, but also to vault whose geometry is assigned by a cloud of points, as that provided for example by a laser scanner survey. This might be of significant interest for practical applications.

Furthermore, recalling (15)-(18), for each point $P_{ij} \in \mathscr{P}$ the numerical counterpart of the constraints that must be satisfied is:

(i) *Equilibrium constraints:*

$$\left[\frac{\partial^2 f}{\partial x^2}\frac{\partial^2 F}{\partial y^2}+\frac{\partial^2 f}{\partial y^2}\frac{\partial^2 F}{\partial x^2}-2\frac{\partial^2 f}{\partial x \partial y}\frac{\partial^2 F}{\partial x \partial y}=q\right]_{P_{ij}} \qquad \forall P_{ij} \in \mathscr{P}, \tag{21}$$

i.e. the unilateral membrane must be in equilibrium with the applied load;

(ii) *Unilateral constraints:*

$$\begin{cases} \left[tr\mathbf{S} \le 0 \quad \& \quad \det\mathbf{S} \ge 0\right]_{P_{ij}} \\ \left[f_{\text{int}} \le f \le f_{ext}\right]_{P_{ij}} \end{cases} \qquad \forall P_{ij} \in \mathscr{P}, \tag{22}$$

i.e. the stress field must be negative semidefinite and the membrane must be contained into the thickness of the vault.

It is worth to note that this way, although the optimization process is conducted with reference to a discrete set of points, we obtain a continuum solution for the unknown functions (f, F), defined by the coefficients of the approximating polynomials.

3.2 Boundary conditions and additional constraints

Boundary value problems governed by PDE equations, like the equilibrium problem for masonry vaults under investigation, require Dirichlet type or Neumann type[2] boundary conditions to be solved.

Anyway, since our approach configures the equilibrium problem in a constrained optimization problem, once specified the objective function (see *Sect. 3.3*) it is always possible to obtain an optimal solution obeying to the assigned constraints without it being strictly necessary to assign any boundary condition. However, from the engineering point of view, boundary conditions might have considerable relevance for obtaining solutions consistent with the actual support conditions of the vault. For example, either free edges or boundary arches or walls able to take and transfer thrusts may occur; clearly, these different support conditions strongly influence the actual distribution of the stresses in the vault.

In order to introduce also boundary conditions in the optimization process (19), it is possible to define a subset $\mathscr{V} \subset \mathscr{I}$ consisting of points belonging to the boundary $\partial\Psi$ of Ψ, where suitable boundary conditions have to be assigned.

Now, in absence of horizontal loads, static-type boundary conditions can easily be imposed through geometrical conditions on the Airy stress function *F*, exploiting the duality between the Airy Stress Function *F* and the membrane geometry *f* expressed by (15) with an approach similar to that in [51]. Such duality transforms geometric conditions to mechanical conditions and, from a practical point of view, satisfying such geometric conditions may be easier than imposing mechanical conditions directly. To this aim it has to be recalled that the curvatures of the surfaces described by the pair of functions *f* and *F* through their second partial derivatives, and that from the definition of the Airy stress function *F* (14) it is clear that the curvature in a generic direction of *F* corresponds to membrane stresses in the orthogonal direction and vice versa. Here, as it is suggested in [52], for masonry vault we consider only two kinds of boundary conditions:

(i) *Free Edge*

both normal and shear stresses are required to vanish along the edge, i.e.:

$$\frac{\partial^2 F}{\partial s^2} = \frac{\partial^2 F}{\partial s\,\partial n} = 0, \tag{23}$$

[2] According to the classical terminology of Partial Differential Equation, a Dirichlet boundary condition consists in assigning the value of the unknown function at the boundary, whereas a Neumann boundary condition specifies the value of a derivative of the unknown function at the boundary.

where $\frac{\partial F}{\partial n}$ and $\frac{\partial F}{\partial s}$ denote the derivatives of F in the directions normal and tangent to the horizontal projection of the edge, respectively;

(ii) *Fixed edge*

both normal and shear stresses along the edge are admitted, due to the interaction between the vault and the edge abutment. In this case, no boundary conditions are added in the optimization process (19), and once solved the problem and then determined the Airy stress function F, $\frac{\partial^2 F}{\partial s^2}$ and $\frac{\partial^2 F}{\partial s \partial n}$ give the support reactions.

Remark: in [52] it is suggested a third kind of boundary condition concerning edges supported by a shear diaphragm; here, only membrane stresses normal to that edge vanish but shear stresses are admitted. For the present problem, this kind of boundary condition cannot be considered because it is not compatible with the unilateral constraints coming from the No-Tension assumption on the material (see (17)).

It is important to underline that in the presence of horizontal loads the direct duality between the membrane stresses projected on the plane (x, y) and the curvature of the Airy stress function is lost, and the definition of boundary conditions on $\partial\Psi$ is more complex.

Notice that instead of static-type boundary conditions it is possible to impose kinematic-type boundary conditions that, in a dual way, directly influence the geometry of the membrane, and then the function f. Thus, if kinematic-type boundary conditions are considered, the search of solutions in terms of purely compressed equilibrium membranes contained within the thickness of the vault is strongly simplified in terms of computational cost. But, in the spirit of the lower bound theorem of Limit Analysis, if optimal solutions corresponding to the best possible estimate of the load-bearing capacity of the masonry vault are searched, the restrictions of the set of possible solutions descending from the imposition of kinematic-type boundary conditions have to be avoided, and (when possible) static-type boundary conditions have to be preferred.

Anyway, kinematic-type boundary conditions may be useful for searching solutions compatible with eventual cracks existing on the vault. Indeed, in real life, it is very common that masonry vaults show cracks usually associated to "hinges" opening; an accurate survey of the vault, preliminary to the structural analysis, may give the information needed for characterizing the position and the extension of cracks.

We recall that for masonry arches if the sliding between blocks does not occur the cracks affect the position of the thrust line [3]. Indeed, the opening of a crack at the intrados (or at the extrados) corresponds to the formation of a hinge in the opposite part of the same cross section of the arch, and then the thrust line is enforced to be tangent to the arch border in the hinge point. Analogously, for masonry vaults it is possible to assume that when a cracking hinge exists, the equilibrium membrane *f* is enforced to pass along particular points. In particular, given the curve formed by the crack, *f* has to be tangent to the extrados or to the intrados of the vault on a curve opposite to the latter with respect to the thickness of the vault.

Thus, for searching by TSM equilibrium solutions consistent with a certain cracked configuration of the vault a reasonable approach is that of defining a subset $\mathscr{C} \subset \mathscr{P}$ of points belonging to the horizontal projection of cracking hinge curves. For each point $P_{ij} \in \mathscr{C}$, it is possible to set:

$$\left[f(x,y) = f_{\text{int}}(x,y) \right]_{\text{P}_{ij}} \quad \text{or} \quad \left[f(x,y) = f_{ext}(x,y) \right]_{\text{P}_{ij}} \qquad \forall P_{ij} \in \mathscr{C}, \tag{24}$$

i.e., to impose that in correspondence of the hinge curves the membrane *f* is tangent to the intrados or to the extrados of the vault, depending on the position of the crack (if the crack is at the intrados, *f* has to be tangent to the extrados, and vice versa). Conversely, pass-through cracks as Sabouret cracks could also be taken into account by suitably dividing the vault in parts, whose equilibrium has to be studied separately.

> *Remark*: it is important to point out that (24) imposes only that at some points the membrane and the extrados or intrados surfaces have to be coincident. However, at the same time, the constraints in (22) impose that the membrane has to be contained between the intrados and the extrados surfaces of the vault. The combination of the above two classes of constraints enforces that the membrane cannot be secant but at most tangent to the extrados and/or the intrados along prescribed lines.

3.3 Objective functions

It is well known that by lower bound theorem of Limit Analysis the existence of an arbitrary statically admissible stress field is a sufficient condition to prove that the vault is “safe” with respect to the assigned load condition, but no information about the “distance” of the considered load condition to the actual collapse loads of the vault are given (i.e., it is not possible to quantify the structural safety level and to determine an accurate estimate of the load-bearing capacity), and the obtained solution may be very conservative.

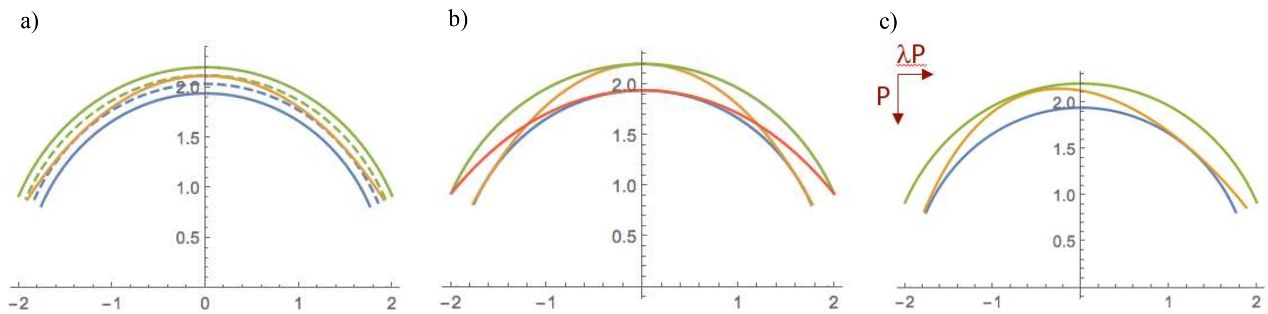

Figure 4. Objective functions: (a) Estimation of the Geometrical Factor of Safety; (b) Determination of the maximum and minimum thrust solutions; (c) lower bound estimation of the collapse multiplier λ_c of a generic live load condition.

With the aim of configuring a method for vaults structural analysis that does not provide solutions in the form of a dichotomous variable (the vault is safe/unsafe) but allows for fully exploring the entire spectrum of the load-bearing capacity of the vault, it is necessary to qualify the obtained solutions or, in other words, to look for extremal or "optimal" solutions.

To this aim, we introduced appropriate objective functions allowing for searching, among the infinite statically admissible solutions complying with the constraint conditions, extremal solutions representative of certain structural conditions (maximum load-bearing capacity, maximum or minimum thrust, etc.) that can be associated with the structural safety level of the vault. In what follows, we give some details about the considered objective functions.

(i) Geometrical Factor of Safety (GFS)

In order to qualify, in terms of structural safety level, solutions obtained by the application of the lower bound theorem of Limit Analysis to masonry arches, Heyman in [16] introduced the concept of Geometrical Factor of Safety (GFS) as the ratio between the actual thickness of the arch and the minimum thickness of an ideal homothetic arch capable of enveloping a possible equilibrium thrust line.

The idea of GFS can be easily extended to masonry vaults: in this case, GFS can be defined as the ratio between the actual thickness of the vault and the minimum thickness of an ideal homothetic vault capable of enveloping a possible equilibrium membrane (Figure 4a). GFS could be considered as representative of the effective load-bearing capacity of the vault with reference to the considered class of loads.

According to the above definition, for determining the GFS by the optimization process, it is possible to employ the following objective function:

$$\sum_{\mathrm{P}_{ij}\in\Psi}\left[f_m\left(x_i,y_j\right)-f\left(x_i,y_j\right)\right]^2, \tag{25}$$

together with the constraints in (21)-(22). This way, as in a least-squared polynomial regression, TSM searches among the infinite statically admissible solutions the purely compressed membrane contained into the thickness of the vault that minimizes the variance between the thrust surface and the middle surface in terms of distances, and thus that minimizes the error function represented by the sum in (25).

(ii) Maximum/Minimum Thrust solution

One of the key aspects of the mechanics of curved masonry structures is that, under an assigned load condition, they generate thrusts on the abutments that support them. The evaluation of this thrust is a very important goal of any structural analysis of masonry vaults but, unfortunately, this is not a problem of a simple solution.

We recall that the maximum thrust can be conservatively considered for the assessment of the structures supporting the vault, whereas the minimum thrust solution is generally considered in the literature as the solution better approximating the actual thrust level of the vault. This, especially for the case of historical constructions, that very likely has suffered from settlements of abutments along the centuries, even of small size [4].

In analogy with the simplest case of the masonry arch, for a masonry vault a different value of thrust on the abutments is associated to each possible equilibrium thrust surface. Clearly, if among all the possible solutions, those corresponding to the minimum and the maximum thrust are determined, it is possible to claim that the actual value of the thrust will lie between these two limit values.

By TSM, the search for solutions corresponding to the maximum and minimum thrust can be performed by introducing a suitable objective function in the optimization process. To this aim, considering only gravitational loads (the problem of the determination of the maximum and minimum thrust on the abutments is relevant right for this load condition), it is reasonable to assume that the forces per unit length transmitted to the abutments are tangent to the thrust surface. Thus, again in analogy with masonry arches, the minimum thrust solution corresponds to the geometric configuration of the membrane with minimum span and maximum rise. Vice versa, to the maximum thrust solution corresponds the maximum span and the minimum rise membrane [4] (Figure 4b).

For the above observations, recalling (13), we define Membrane Projection Factor (*MPF*) in a given point the ratio between the area of the membrane and its projection on the plane (x, y):

$$MPF = \frac{\sqrt{1 - \sin^2\phi \sin^2\theta}}{\cos\phi \cos\theta}, \tag{26}$$

where $\cos\phi$ and $\cos\theta$ could be expressed in terms of f by (9). Now, in order to search for maximum and minimum thrust solutions, it is sufficient to consider in the optimization process that the objective function to be minimized (or maximized) is:

$$\sum_{\mathrm{P}_{ij} \in \partial\Psi^r} MPF, \tag{27}$$

i.e., the sum of the values of *MPF* for points belonging to the neighborhood of the restrained boundary $\partial\Psi^r$ of the horizontal projection Ψ of the vault. Indeed, it is clear that the membrane solution that minimizes (27) corresponds to the thrust surface with the smallest slope with respect to the horizontal plane (x, y) and thus related to the maximum thrust. On the contrary, for the membrane solution maximizing (27), related to the minimum thrust (Figure 4b).

For more complex problems (for example not fully-supported conditions like in presence of openings, horizontal loads, etc.), suitable objective functions aimed at obtaining the minimum or the maximum thrust solution could be drowned up and implemented in the framework of TSM[3]. For instance, the objective function (27) works fine if the chosen grid is perfectly regular (points equally spaced). Analyzing vaults for which no symmetry in the geometric description is present, could be useful to use different distribution of points. In this case, it would be better to add something suitable for weighting areas coming from irregular grids. E.g., if something linked to the tributary area is assumed in the expression, the objective function for uniform grid becomes exactly Eq 27, whilst it can take into account irregular grids.

(iii) Lower bound estimation of collapse loads

The possibilities offered by the Limit Analysis, and, in particular, by the application of the lower bound theorem, are not limited to the safety evaluation of a structure with respect to a fixed load condition. Rather, a result of greater interest is represented by the possibility of obtaining an estimate, as accurate as possible, of the load factor that could lead to the collapse of the structure under an assigned monotonic loading process.

For applying the above concepts to the present case of masonry vaults, let's consider a linear loading process in the form:

$$\overline{p}\left(x,y,\lambda\right)=\overline{p}_0(x,y)+\lambda\overline{p}_1(x,y), \tag{28}$$

where $\overline{p}_0\left(x,y\right)$ is a dead load distribution (for example, the self-weight), $\overline{p}_1\left(x,y\right)$ is a live load distribution (either vertical or horizontal) and λ is a load multiplier; in (29), loads refer to the planar projection of the vault.

Now, suppose that for $\lambda=0$ there exists an admissible equilibrium solution, and let λ_c be the actual value of the collapse load multiplier in the loading process (28). In order to determine the best lower bound estimate of λ_c, it is possible to employ TSM in the following way.

In the optimization process, for a given load condition the objective function (25) allows for determining the "safest" possible thrust surface, i.e., the equilibrium thrust surface closest to the middle surface. With reference to the loading process (28), if we iteratively repeat the analysis by increasing at each iteration the value of the load factor λ and by considering the objective function (25), we determine a series of "safest" possible thrust surfaces that gradually pull away from the middle surface. The limit condition is reached for the load factor λ corresponding to a "safest" thrust surface tangent to the intrados and/or to the extrados of the vault: this case corresponds to a load multiplier for which GFS = 1 (Figure 4c). In this vein, horizontal

[3] The objective function (27) is suitable in case of regular grids (points equally spaced). However, without lack of generality, in some cases like, for example, asymmetric vaults, it may be appropriate to employ grids with an irregular distribution of points. In these cases, it would be better to generalize the expression of the objective function introducing something suitable for weighting areas coming from irregular grids. Notice that if this generalization is made by expression linked to the tributary area, then an objective function convenient for irregular grids is obtained, that reduces exactly to (27) in case of uniform grids.

live loads proportional to the self-weight may be used for representing the maxima inertial effects related to the seismic actions, and then for studying of the seismic capacity of the vault.

In this context, it is interesting to point out that TSM can be also employed for gathering information about possible collapse mechanisms under an assigned loading processes: this could be very useful since, contrary to the case of masonry arches, there is still a lack of knowledge about collapse mechanisms of masonry vaults.

In order to exploit the capabilities of TSM in identifying potential collapse mechanisms, it is possible to follow an approach similar to that proposed in [16] for masonry arches. In the latter case, in a linear loading process like (28) the collapse limit condition associated with the highest value of λ that satisfies the lower bound theorem of Limit Analysis corresponds to a (unique) thrust line still contained into the thickness of the arch, but tangent to the intrados and to the extrados in a certain number of points (Figure 4c). The kinematic counterpart of the above is that the collapse mechanism will be based on the formation of hinges in correspondence of these tangency points [4].

In the same way, for masonry vaults the iterative application of TSM described just above leads to identify some tangency curves between the limit thrust surface and the intrados or the extrados of the vault; these tangency curves identify possible (spatial) hinges and then may give a characterization of the possible collapse mechanism of the vault under the considered loading process.

3.4 Polynomial approximation

The above-mentioned optimization problem, also in presence of very restrictive constraints (*Sect. 3.1-3.2*), both geometrical (the membrane must be contained within the thickness of the vault) and mechanical (the generalized membrane stress tensor **S** must be negative semidefinite), like all problems of optimal control of systems with distributed parameters or governed by partial differential equations, is strongly undetermined and might have many extremal solutions. Therefore, it is practically impossible to determine a closed-form solution.

For the search of numerical solutions, a polynomial approximation of the unknown functions is a very helpful approach for reducing the variables of the problem to a reasonable number [53] by constraining, in fact, the search for a solution to a finite dimensional subspace of functions.

Since according to *Sect. 2* the equilibrium problem for masonry vaults has been reduced from $\mathbb{R}^3$ to $\mathbb{R}^2$, it is possible to approximate the pair of unknown scalars functions of the problem (*f, F*) in the following polynomial form:

$$\begin{cases} f(x,y) = \sum_{j=0}^{n} \sum_{i=0}^{j} \alpha_{ij} x^i y^{j-i} \\ F(x,y) = \sum_{j=0}^{n} \sum_{i=0}^{j} \beta_{ij} x^i y^{j-i}, \end{cases} \tag{30}$$

where α_{ij} and β_{ij} are real coefficients and *n* is the polynomial degree. Here we assume that both the unknown functions can be expressed by polynomials of the same degree *n*.

Therefore, the optimization problem (19) reduces to the determination of the optimal values of α_{ij} and β_{ij} coefficients, which are now the variables.

In this form, the above problem is then declined as a form-finding problem [51,54] of a unilateral membrane subject to mechanical and geometrical constraints.

> *Remark*: The degree of polynomials (30) can be chosen according to the complexity of the geometry of the analyzed vault and of the considered load condition. Complex vault geometries or load conditions could require polynomial approximations of a higher degree to reach reasonable statically admissible solutions due to the higher complexity of the membrane geometry: this considerably affects the computational cost of the process. In practical applications, it might be useful a sensitivity analysis aimed at finding the best compromise between computational costs and accuracy of the approximation.

3.5 Optimization algorithms

The above-stated optimization problem involves many independent variables, i.e., the coefficients α_{ij} and β_{ij} defining the polynomial approximation of the couple of unknown functions *(f, F)*, and several nonlinear equality and inequality constraints. For these reasons, we may expect all kinds of mathematical tricks: multi-extremality, singularity, noise i.e. the inaccuracy in the solution evaluation and so on. In this case, we cannot use properly the concepts of gradient and of sensitivity [53].

Because of these shortcomings, classical Gradient-Based methods that use first-derivatives (or gradient) and/or second derivatives (Hessian) hardly apply successfully. Rather, algorithms known as Direct Methods or Derivative-Free Optimization (DFO) methods [55] making use of function values at a set of sample points to determine a new iterate without attempting to calculating or approximating the gradient seem to be more useful.

Widely used DFO methods include deterministic approaches as the simplex-reflection method by Nelder and Mead, conjugate-direction methods [55], or non-deterministic and stochastic approaches as Simulated Annealing, Genetic Algorithms, and Differential Evolution.

For the purpose of the present paper, we have implemented the TSM algorithm in Wolfram Mathematica 11.1 environment, and we have tested the effectiveness in the calculations of both Nelder-Mead [55] and Differential Evolution [56] optimization strategies.

Notice that by using DFO methods (also implemented in the optimization package of Mathematica) it is not possible to guarantee that the procedure leads to the global optimum. This point deserves more study since in many cases the attraction domain of local extrema is much larger than the attraction domain of global extrema. Moreover, each problem has to be considered as multi-extremal unless the opposite statement is proved [53].

By a number of numerical experiments we have observed that, although Nelder-Mead method has shown a better efficiency in terms of computational effort in some simpler applications, the Differential Evolution method overall manage better the problem, even in more complex cases: it has proved to be relatively robust and to work well also for problems with multiple local minima [56]. Thus, we have chosen the Differential Evolution method as the optimization solver for the problem (19).

In *Sect. 5*, by referring to analytical and experimental results in the literature, we will discuss and validate the effectiveness and the accuracy of TSM results and we will also report the required computational costs.

4. Overview of the main steps of the Thrust Surface Method

After an in-depth description of the method, in this Section, we will summarize the main steps of TSM, that configure a practical tool for the lower bound Limit Analysis of masonry vaults of any geometry subject to arbitrary load conditions.

a) Definition of the geometry of the vault

The geometry of the vault must be expressed in the implicit form (Monge patch). To this aim, it is necessary to assign the expressions of intrados f_{int}, extrados f_{ext} and middle surface f_m functions.

For vaults with a complex geometry and/or affected by cracks and deformations, for which the analytical description of the geometry is very difficult, it is possible to approximate the actual geometry by using classic polynomial interpolation methods starting, for example, from a cloud of points obtained by a laser scanner survey.

b) Assignment of the loads

In the assignment of loads, for the purpose of Limit Analysis, it is necessary to distinguish the dead load component $\overline{p}_0(x,y)$ from the live load component $\overline{p}_1(x,y)$ that is increased from zero by a load multiplier λ.

Loads must be assigned as forces per unit of area of the horizontal projection of the vault Ψ.

c) Choice of the grid of points and of the degree of the approximating polynomials

In the domain Ψ of the projection of the vault on the plane (x,y), it is first necessary to define the set of points $\mathscr{P}$ for which the input data of the problem will be assigned (geometry and load conditions). Then, it is necessary to define the degree of the polynomials (30) approximating the unknown functions (*f, F*).

Both choices are related to the complexity of the geometry of the vault and of the assigned load condition: the more the problem is complex, the higher should be the degree of the approximating polynomials and the number of points constituting the set $\mathscr{P}$.

Moreover, if the geometry and/or the loading conditions present singularities (for example, folded surface or jumps in the load condition) it is advisable for $\mathscr{P}$ to contain the points belonging to the horizontal projection of the singularity curves. In these cases, it may be convenient also to employ piecewise defined approximating polynomials (see *Sect. 5.3*).

d) Assignment of the constraints

As it is pointed out in *Sect. 3.1*, for each point of the set $\mathscr{P}$ it is necessary to impose the constraint conditions expressing the equilibrium requirement and the No-Tension assumption of the material.

e) Assignment of the boundary conditions and of additions conditions

Even if not strictly necessary for solving the problem, in order to determine solutions more compliant with the features of the specific problem under investigation, it is possible to impose boundary conditions, which will be assigned for the points of the subsets $\mathscr{V}$ of $\mathscr{P}$.

Also additional conditions can be introduced, as for example those enforcing that the membrane solution is compatible with cracking hinges observed in the survey of the vault, see *Sect. 3.2*.

f) Choice of the objective function and solution of the equilibrium problem

According to the aim of the analysis, it is possible to choose among the objective functions (25)-(27) introduced in *Sect. 3.3*.

At the end of the optimization process TSM provides as the result the coefficients α_{ij} and β_{ij} defining the polynomial approximation of the couple of unknown functions *(f, F).* This way, a continuous statically admissible solution for the three-dimensional equilibrium problem for a masonry vault is found.

5. Case studies

In this Section, the application of the Thrust Surface Method (TSM) to masonry vaults having two different geometries, a barrel vault and a cross vault, will be illustrated and discusses in comparison with results available in the literature. This allows us to validate the proposed innovative approach, and for highlighting its effectiveness in the assessment of the load-bearing capacity of masonry vaults. Moreover, TSM results suggest useful information for understanding the complex three-dimensional behavior that these structures exhibit.

In particular, the examined case studies are “theoretical” vaults, whose geometry is not given by the survey of real-life constructions; anyway, the considered dimensions are consistent with typical dimensions of true vaults. In particular, *Sect. 5.2* is devoted to the application of TSM to a barrel vault, whereas *Sect. 5.3* concerns a cross vault.

The employ of the different objective functions introduced in *Sect. 3.3* allows for determining the GFS, and maximum/minimum thrust solutions.

5.1 Loading conditions

For both the vaults analyzed in the following we study the load-bearing capacity only with respect to the self-weight, without live loads. Thus, we consider the loading case:

$$\overline{p}(x,y) = \overline{p}_0(x,y), \tag{31}$$

where the dead load $\overline{p}_0(x,y) \equiv \overline{p}_z(x,y)$ acts in the z-direction.

The choice of not consider loads like the weight of the infill or live loads (easily implementable in the TSM algorithm) is motivated by the purpose of the following analyses, that is the validation of the proposed innovative approach by the comparison to other analytical, numerical and experimental results in the literature, usually considering only the simple load condition of the self-weight.

In this vein, it has to be pointed out that in most of the approaches in the literature [38,39,57] the self-weight is represented by a uniformly distributed system of forces on the horizontal projection of the vault. We observe that such a system of forces is sufficiently representative of the self-weight only for shallow vaults. For vaults having the geometries that often characterize the historical architectural heritage this approximation is not always acceptable. With the aim of a more accurate description of the forces involved in the equilibrium problem, given the geometry of the middle surface of the vault $f_m(x,y)$ and recalling (13) it is possible to represent the dead load corresponding to the self-weight of the vault for unit area of the horizontal projection Ψ of the vault as follows:

$$\overline{p}_z = \gamma s \frac{\sqrt{1-\sin^2\phi \sin^2\theta}}{\cos\phi\cos\theta}, \tag{32}$$

where γ is the specific weight of the masonry, s is the thickness of the vault and, by (9):

$$\cos\phi = \frac{1}{\sqrt{1+\left(\dfrac{\partial f_m}{\partial x}\right)^2}}; \quad \cos\theta = \frac{1}{\sqrt{1+\left(\dfrac{\partial f_m}{\partial y}\right)^2}}, \tag{33}$$

being θ and ϕ the angles that the middle surface f_m forms with the x and y-axes, respectively.

Clearly, by (32) the load associated with the self-weight is not constant on the horizontal projection of the vault, but it assumes a curvilinear distribution characterized by an inverted profile with respect to the middle surface profile (Figure 5).

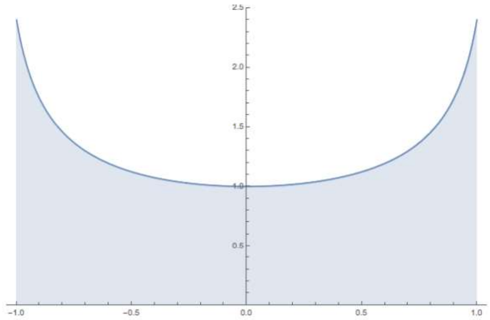

Figure 5. Representation of the self-weight projected on the horizontal plane for a barrel vault.

For computing the self-weight, in both the examined case studies we consider a masonry specific weight $\gamma = 16\ \text{kN/m}^3$.

5.2 Barrel vault

The barrel vault is the simplest vaulted roof system; it is generally used to cover square or rectangular spaces. From the geometric point of view, a barrel vault is characterized as a translation surface with single curvature usually having a semi-circular or segmental profile.

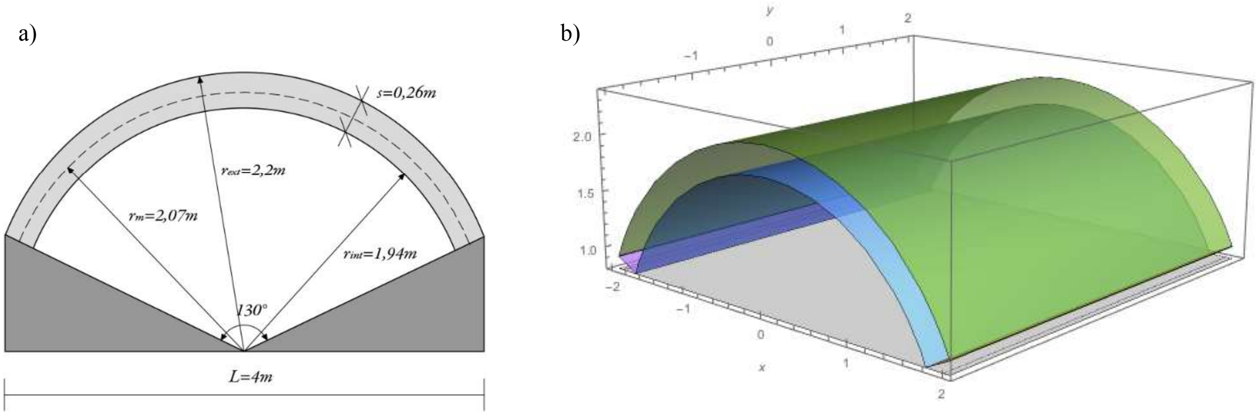

Figure 6. Geometrical description of the studied barrel vault: (a) section of the vault; (b) intrados and extrados surfaces of the vault

For the purposes of the present analysis, we consider a barrel vault on a square plan with a segmental profile of width 130° and a thickness/radius ratio of 12.5%, whose geometric characteristics are shown in Figure 6.

The geometry of the vault can be described *a la Monge* by the following functions:

$$\begin{aligned} f_{\text{int}}(x,y) &= \sqrt{(r_m - s/2)^2 - x^2}, \\ f_m(x,y) &= \sqrt{r_m^{\,2} - x^2}, \\ f_{ext}(x,y) &= \sqrt{(r_m + s/2)^2 - x^2}, \end{aligned} \tag{34}$$

being $f_{int}(x,y)$, $f_m(x,y)$ and $f_{ext}(x,y)$ the intrados, the middle and the extrados surfaces of the vault, respectively, r_m the radius of the middle surface directrix and s the thickness of the vault. Here, *y*-direction coincides with the direction of the generatrix of the vault and the origin of the reference system is the center of the plan of the vault.

In order to assess the effectiveness and the limitations of TSM also from the point of view of the computational cost, for both the polynomial (30) approximating the pair of unknown scalars functions (*f, F*), the degree *n*=4 has been chosen as a compromise between the accuracy and the computational time needed for the calculations. Furthermore, on the horizontal projection of the vault Ψ, the set of points $\mathscr{P}$ has been defined through a square mesh with spacing $r_m/8$.

To make possible comparisons between TSM solutions and other results available in the literature, we considered the case of a barrel vault simply supported by impost walls, neglecting the possible presence of infill walls supporting the head arches. Then, for the points belonging to the horizontal projection of the head arches the following boundary conditions have been imposed:

$$\bar{N}_y = \frac{\partial^2 F}{\partial x^2} = 0 \text{ and } \bar{N}_{xy} = \frac{\partial^2 F}{\partial x \partial y} = 0 \quad \forall \mathrm{P}_{ij} \in |y| = L/2. \tag{35}$$

From the mechanical point of view, (35) means that normal and shear membrane stresses along the head arches vanish.

(i) Geometrical Factor of Safety

By performing TSM analysis under the self-weight of the vault expressed by (32) and by selecting the objective function (25), the optimization process has provided the following polynomial approximation of the two unknown functions (*f, F*) for the solution that maximizes the Geometrical Factor of Safety (GFS):

$$\begin{cases} f(x,y) = 2.110 + 4.689 \cdot 10^{-4} x - 2.986 \cdot 10^{-1} x^2 - 2.070 \cdot 10^{-8} x^3 - 0.011 x^4 \\ F(x,y) = 13.265 + 5.829 \cdot 10^{-7} y - 3.316 y^2 - 1.457 \cdot 10^{-7} y^3 - 5.380 \cdot 10^{-7} y^4, \end{cases} \tag{36}$$

where $f(x,y)$ and $F(x,y)$ are expressed in [m] and [kNm], respectively.

Figure 7a shows in orange the obtained unilateral membrane *f*, that is entirely contained between the intrados (in light blue) and the extrados (in green) of the vault; the graph of the related Airy stress function *F* is displayed in Figure 7b.

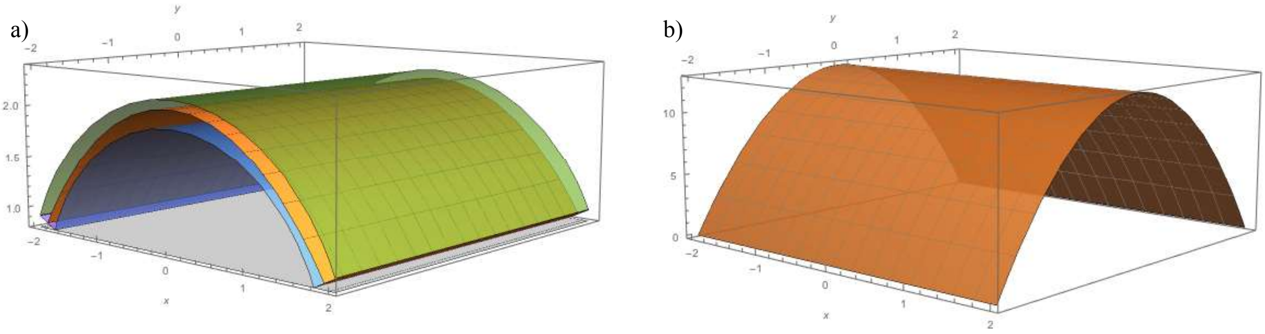

Figure 7. Estimation of the Geometrical Factor of Safety: (a) the unilateral membrane *f*; (b) the Airy stress function *F*.

It is interesting to note that to a barrel vault having an axial development in the *y*-direction corresponds a dual Airy stress function whose graph is characterized by a similar geometry (close to that of a barrel vault), but having an axial development in the orthogonal *x*-direction. This is not surprising, as it is a consequence of the duality discussed in *Section 3*.

The existence of such solution, in view of the lower bound theorem of Limit Analysis, shows that the vault is "stable" under its self-weight, and then the collapse can never occur under this load. By enveloping the obtained membrane by the minimum thickness ideal barrel vault homothetic to the assigned barrel vault, it is found that the obtained solution corresponds to a *GFS* equal to 3.46 (Figure 8). Moreover, with reference to the obtained solution, the horizontal thrust at the imposts is $H = 6.63\ \mathrm{kN/m}$ and the corresponding vertical reaction is $V = 9.62\ \mathrm{kN/m}$.

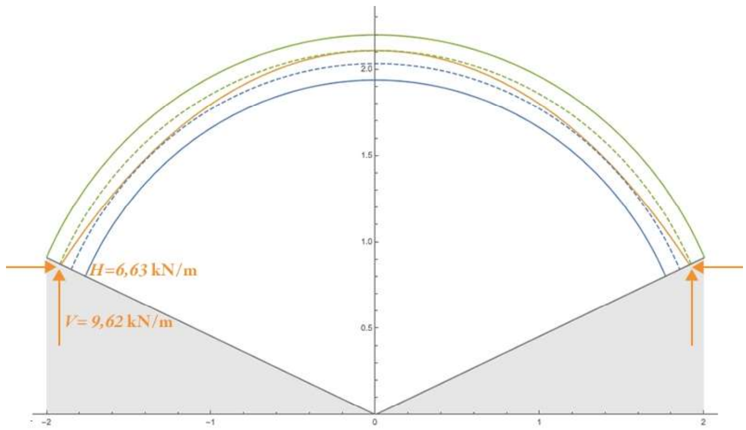

Figure 8. Generic cross section of the vault, entity of the GFS and corresponding horizontal and vertical reactions at supports.

If the Airy stress function *F* is known (rather, it is known its polynomial approximation $(37)_2$) it is possible to obtain by partial derivation (see (14)) the expression of the membrane stresses projected on the plane (x, y). Then, the true membrane stresses can be calculated by (8).

The obtained results in terms of membrane stresses for the maximum GFS solution are represented in Figure 9a-b. Since the stresses N_y and N_{xy} are everywhere zero (Figure 9a), the mechanical behavior of a barrel vault subject to the self-weight can be schematized as a series of parallel compressed arches, arranged orthogonally to the generatrix axis of the vault. No interactions between arches in the direction orthogonal to their planes occur (Figure 9b).

For the above, the obtained solution can be compared with well-known classic Limit Analysis solutions for masonry arches reported in the literature [4,58,59] or with the solution obtainable by applying new numerical approaches for the lower bound Limit Analysis of masonry arches [4,59–61]. In particular, the determined value of GFS is a reliable lower bound of the GFS obtainable by computing the minimum thickness to radius ratio for arches subject only to the self-weight and with a segmental profile of width 130°; indeed, according to [4,58,59], we get $\left(\dfrac{s}{r_m}\right)_{\min} = 0.034$. By dividing the thickness of the considered vault by the obtained value of GFS we may evaluate the minimum thickness of the vault according to TSM; by further dividing by the radius, we get a minimum thickness to radius ratio $\left(\dfrac{s}{r_m}\right)_{\min} = 0.036$, very close with the reference value reported above.

For the validation of TSM results consider also that, since the symmetry, the vertical reaction V at the abutments can be analytically evaluated as:

$$V = \gamma A = \gamma \iint_A dA = \gamma \int_0^{\alpha} d\phi \int_{r_{\mathrm{int}}}^{r_{ext}} \rho \, d\rho = \gamma \frac{\alpha}{2}\left(r_{ext}^2 - r_{\mathrm{int}}^2\right), \tag{38}$$

where A is the area of the half-arch, α is the half angle of embrace of the arch, and ρ is the radial distance of any given point within the arch from the origin O of the coordinate system. Substituting the geometrical parameters in Figure 6, it results $V = 9.80$ kN/m. The value estimated by TSM $V = 9.62$ kN/m has an error only of 1.74%.

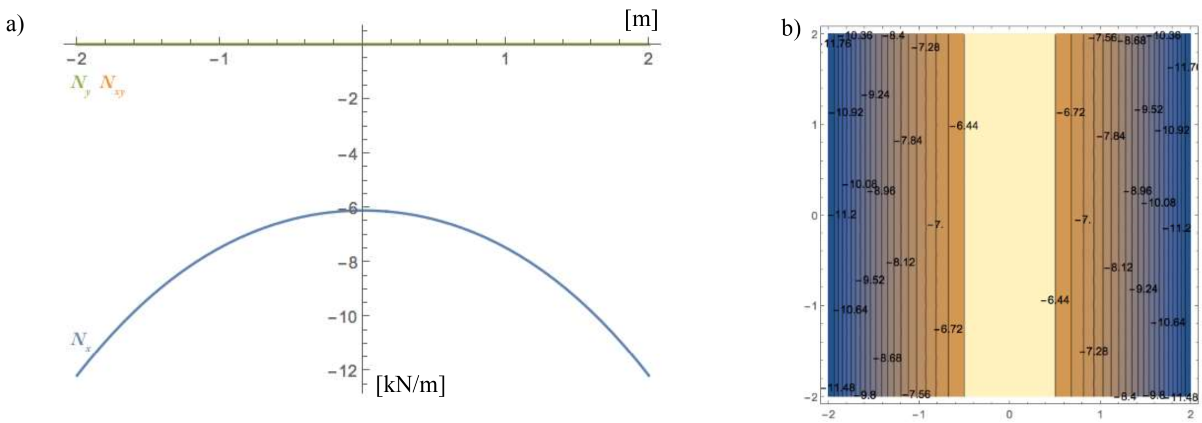

Figure 9. Admissible stress field corresponding to maximum GFS: (a) entity of N_x, N_y and N_{xy} [kN/m] in a generic section of the vault; (b) distribution of N_x [kN/m].

(ii) Maximum and minimum thrust solutions

Again, for the case of the self-weight (32) as the only load, by applying TSM it is also possible to provide an estimation of the maximum and minimum thrusts at the imposts if the objective function (27) is employed.

This way, the obtained maximum thrust solution is expressed in terms of the two unknown functions (*f, F*) by the following polynomial approximations:

$$\begin{cases} f(x,y) = 1.94 - 1.387\cdot 10^{-6}x - 2.204\cdot 10^{-1}x^2 - 1.193\cdot 10^{-8}x^3 - 8.844\cdot 10^{-3}x^4 \\ F(x,y) = 18.095 + 4.058\cdot 10^{-6}y - 4.524y^2 - 1.015\cdot 10^{-6}y^3 - 1.439\cdot 10^{-8}y^4. \end{cases} \tag{39}$$

The shape of the maximum thrust equilibrium membrane (in orange) is shown Figure 10a, and of course is contained between the intrados surface (in light blue) and the extrados surface (in green) of the vault.

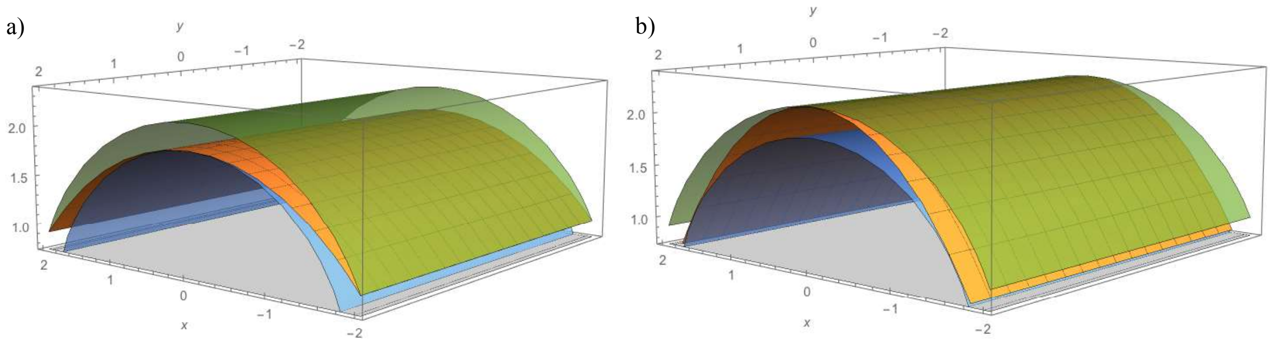

Figure 10. (a) Maximum thrust solution; (b) minimum thrust solution

On the other hand, the polynomial approximation of the two unknown functions (*f, F*) for the minimum thrust solution is:

$$\begin{cases} f(x,y) = 2.200 + 1.432\cdot 10^{-6}x - 3.750\cdot 10^{-1}x^2 - 8{,}014\cdot 10^{-9}x^3 - 2.166\cdot 10^{-2}x^4 \\ F(x,y) = 9.989 - 1.857\cdot 10^{-8}y - 2.497y^2 + 4.642\cdot 10^{-9}y^3 - 5.679\cdot 10^{-9}y^4. \end{cases} \tag{40}$$

The minimum thrust equilibrium membrane (in orange) laying between the intrados surface (in light blue) and the extrados surface (in green) of the vault is depicted in Figure 10b. In (37) and (38) $f(x,y)$ and $F(x,y)$ are expressed again in [m] and [kNm], respectively.

As described for the case of the maximum GFS solution, by partial derivatives of the determined Airy stress function *F* (see (14)), it is possible to evaluate the stress state of the barrel vault in correspondence to the minimum and maximum thrust configurations; then, from the membrane stresses it is possible to calculate the minimum and maximum value of the horizontal thrust H at the imposts. In particular, we get $H_{max} = 9.05$ kN/m for the maximum thrust solution and $H_{min} = 4.99$ kN/m for the minimum thrust solution; this implies that the actual value of the horizontal thrust H on the abutments must be such that $4.99 \text{ kN/m} \le H \le 9.05 \text{ kN/m}$.

Similarly to what has been previously observed for the maximum GFS solution, it is possible to compare the obtained results with maximum and minimum thrust line solutions for masonry arches having the same planar section of the directrix section of the considered vault. By this comparison, as it is evident from Figure 11, the thrust surfaces determined by TSM as well as the results in terms of thrusts are perfectly in agreement with well-known results in the literature relative to masonry arches in [4] (see *Appendix A*).

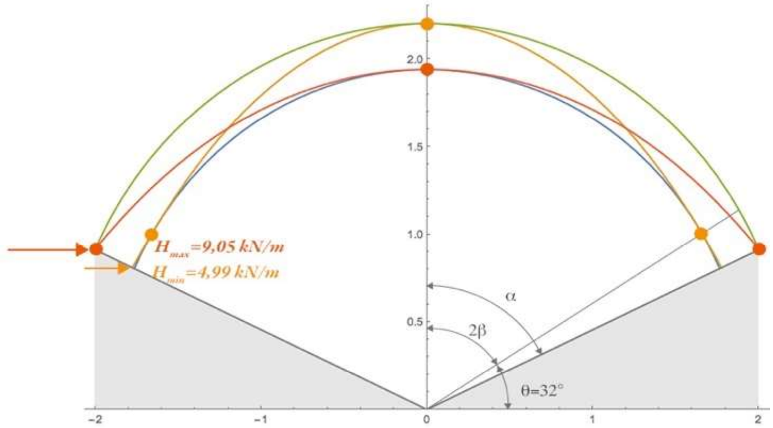

Figure 11. Minimum thrust (yellow) and maximum thrust (red) solutions in a section of the case study vault.

Although TSM represents an application of the lower bound theorem of Limit Analysis, by virtue of the methodology used, that allows for determining optimal solutions, it is also possible to obtain kinematic information about potential collapse mechanisms. Indeed, in analogy with the thrust line analysis for masonry arches, it is possible to associate the tangency curves between the thrust surface and the intrados or the extrados of the vault to the formation of cracking hinges. We observe that the position of the cylindrical hinges in the maximum and minimum thrust configurations found by TSM are in perfect agreement with analytical [4,59] and experimental [62] results in the literature, and with crack patterns usually observed in many real-life case studies of barrel vaults.

Notice that the minimum thrust solution suggests the formation of the classic extrados hinge at the keystone and intrados hinges at the haunch typical of barrel vaults (or an arches) on spreading supports [63], and thus in the minimum thrust condition. For the sake of the completeness, the obtained position of intrados hinges at $\theta = 32°$ (Figure 11) is in perfect agreement with the results in [4,59].

Finally, for what concerns the computational costs, the above analyses have been completed in 25 s by using a common personal computer Intel Core I7-4770 equipped with 16GB of RAM.

5.3 Cross vault

We consider a cross vault with a square plan. From the geometrical point of view it is possible to think the vault as obtained from the intersection of two orthogonal barrel vaults having the same geometry of that examined in *Sect. 5.2*. In particular, the geometry is singular in correspondence of the diagonals, and it can be described by the following piecewise defined functions:

$$
f_{\text{int}}(x,y)=\begin{cases}\sqrt{(r-s/2)^2-y^2} & |x|\geq|y|\\ \sqrt{(r-s/2)^2-x^2} & |x|<|y|\end{cases}
$$
$$
f_m(x,y)=\begin{cases}\sqrt{r^2-y^2} & |x|\geq|y|\\ \sqrt{r^2-x^2} & |x|<|y|\end{cases} \tag{41}
$$
$$
f_{ext}(x,y)=\begin{cases}\sqrt{(r+s/2)^2-y^2} & |x|\geq|y|\\ \sqrt{(r+s/2)^2-x^2} & |x|<|y|,\end{cases}
$$

describing the intrados surface, the middle surface, and the extrados surface, respectively (Figure 12).

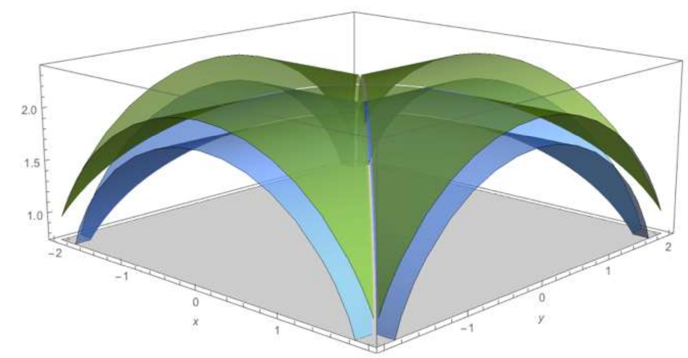

Figure 12. Intrados and extrados surfaces of the vault

In this case, given the complexity of the geometry, the search of a smooth unilateral membrane entirely contained within the thickness of the vault becomes very difficult and would requires a very fine discretization of the domain Ψ of the horizontal projection of the vault and the employ of approximating polynomials (30) of very high degree. This way, the computational cost would result very high. Moreover, the obtainable smooth solution would not reflect the geometric characteristics of the shape of the vault, which indeed presents singularity curves at diagonals.

For these reasons, since the singularity of the geometry, we prefer to assume that the admissible stress field is singular at diagonals too. This implies that both the membrane *f* and the Airy stress *F* are continuous non-smooth functions.

In particular, by following the approach in [44], we consider that the pair of unknown functions *(f, F)* are both piecewise functions, singular along the same curves Γ_1 and Γ_2 (Figure 13), corresponding to the horizontal projection of the fold lines of the vault. This means that statically admissible stress fields will admit Dirac-delta singularity on Γ_1 and Γ_2. Notice that if *F* is singular on one curve Γ, then also *f* must be singular on the same curve, as it is proved in [38].

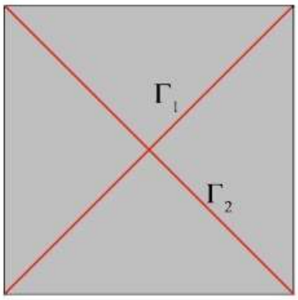

Figure 13. Singularity line Γ_1 and Γ_2 on the horizontal projection Ψ of the vault corresponding to the vault folds.

For what concerns the approximating polynomials of (*f, F*), the above assumption yield that these polynomials can be expressed in the following piecewise defined form:

$$f(x,y) = \begin{cases} \sum_{j=0}^{n}\sum_{i=0}^{j} \alpha_{ij} x^i y^{j-i} & |x| \geq |y| \\ \sum_{j=0}^{n}\sum_{i=0}^{j} \beta_{ij} x^i y^{j-i} & |x| < |y| \end{cases}$$
$$F(x,y) = \begin{cases} \sum_{j=0}^{n}\sum_{i=0}^{j} \gamma_{ij} x^i y^{j-i} & |x| \geq |y| \\ \sum_{j=0}^{n}\sum_{i=0}^{j} \delta_{ij} x^i y^{j-i} & |x| < |y|, \end{cases} \tag{42}$$

with obvious meaning of the symbols.

Now, it becomes necessary to add in the optimization process additional constraints representing the continuity conditions of the unknown functions (*f, F*) at the two diagonal curves Γ_1 and Γ_2, that are:

$$\begin{cases} \sum_{j=0}^{n}\sum_{i=0}^{j} \alpha_{ij} x^i y^{j-i} = \sum_{j=0}^{n}\sum_{i=0}^{j} \beta_{ij} x^i y^{j-i} & \forall P_{ij} \in \Gamma_1, \Gamma_2 \\ \sum_{j=0}^{n}\sum_{i=0}^{j} \gamma_{ij} x^i y^{j-i} = \sum_{j=0}^{n}\sum_{i=0}^{j} \delta_{ij} x^i y^{j-i} & \forall P_{ij} \in \Gamma_1, \Gamma_2. \end{cases} \tag{43}$$

By admitting singularities for the unknown functions (*f, F*), it is simpler to achieve sufficiently representative results with approximating polynomials of low degree and with a discretization of the horizontal projection of the vault not much dense. In particular, we use polynomials of degree $n = 4$ and we define the set of points $\mathscr{P}$ on Ψ with a square mesh having a spacing equal to $r_m / 8$.

About the boundary conditions, for the purposes of the comparison with the results in the literature, we considered a cross vault simply supported at corners, neglecting the presence of infill walls at the four sides. This free-edges assumption for side arches of the vault implies the impossibility to transfer normal and shear stresses along the perimeter edges of the horizontal projection of the vault Ψ. Such conditions are satisfied if the Airy stress function F is constant along the boundary of Ψ:

$$F = const \qquad \forall \mathrm{P}_{ij} \in \mathscr{V}. \tag{44}$$

(i) Geometrical Factor of Safety

With reference to the only self-weight (32), by using TSM it is possible to determine the polynomial approximations of the pair of unknown functions (*f, F*) representing the solution of the equilibrium problem corresponding to the maximum GFS; to this aim, the objective function in (25) has to be considered.

In Figure 14a it is shown in orange the obtained unilateral membrane *f* entirely contained between the (in light blue) and the extrados (in green) of the vault, while Figure 14b shows the graph of the dual Airy stress function *F*.

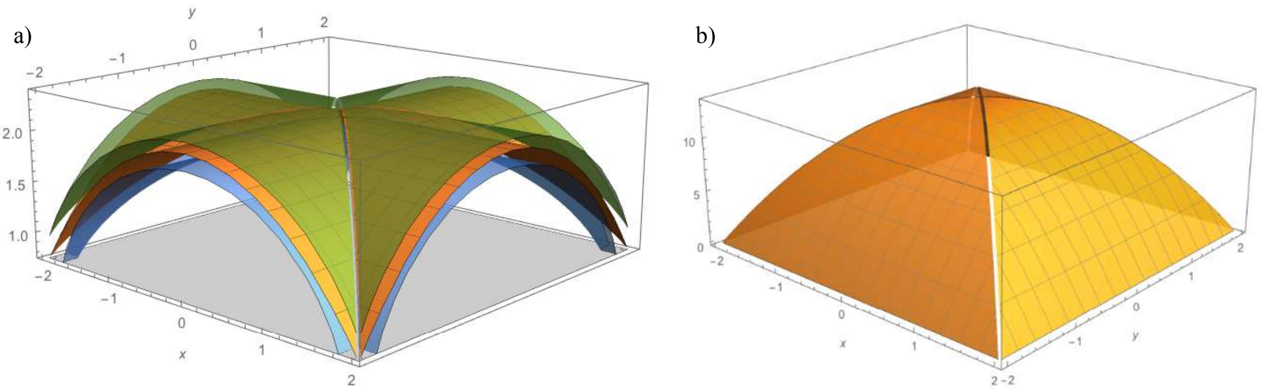

Figure 14. Estimation of the Geometrical Factor of Safety: (b) the unilateral membrane *f* entirely contained between intrados and extrados surfaces of the vault; (b) the dual Airy stress function *F*.

It is possible to observe the interesting geometric analogy between the shape of the membrane and the shape of the graph of the stress function. Indeed, in analogy with the results obtained in [38], to a "cross-shaped" membrane corresponds an Airy function that presents the typical shape of a pavilion vault. This duality expresses the close relationship between form and structure that strongly characterizes 3D masonry structures.

By enveloping the obtained membrane by the minimum thickness ideal cross vault homothetic to the assigned cross vault, it is possible to determine a GFS equal to 3.52.

From partial derivation of the determined Airy stress function *F*, it is possible to obtain by (14) the membrane stresses projected on the horizontal plane (x, y). It can be noticed that shear stresses $\bar{N}_{xy}$ are everywhere zero, while normal stresses $\bar{N}_x$ and $\bar{N}_y$ jump over singularity lines Γ_1 and Γ_2 (Figure 15a-b).

a) b)

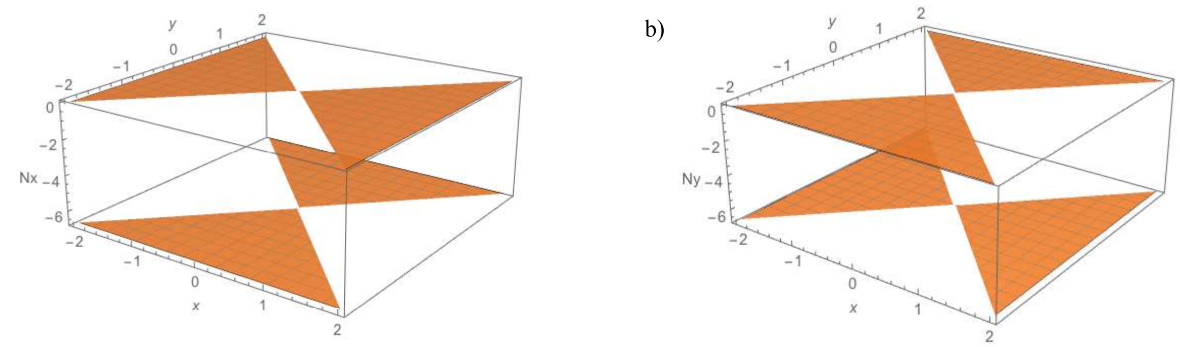

Figure 15. Projected membrane stresses on the horizontal plane: (a) $\bar{N}_x$ [kN/m]; (b) $\bar{N}_y$ [kN/m].

Recalling (6), the obtained statically admissible stress field **S** can be expressed by the following sum:

$$\mathbf{S} = \mathbf{S}_r + \mathbf{S}_s, \tag{45}$$

where $\mathbf{S}_r$ is the regular part describing membrane stresses within the four webbings of the vault, and related to the second-order partial derivatives of the Airy stress function F:

$$\mathbf{S}_r = \begin{pmatrix} \dfrac{\partial^2 F}{\partial y^2} & -\dfrac{\partial^2 F}{\partial x \partial y} \\ -\dfrac{\partial^2 F}{\partial x \partial y} & \dfrac{\partial^2 F}{\partial x^2} \end{pmatrix}, \tag{46}$$

and $\mathbf{S}_s$ is the singular part concentered on the two diagonals Γ_1 and Γ_2:

$$\mathbf{S}_s = N(\Gamma_1)\delta(\Gamma_1)\mathbf{t}_1 \otimes \mathbf{t}_1 + N(\Gamma_2)\delta(\Gamma_2)\mathbf{t}_2 \otimes \mathbf{t}_2, \tag{47}$$

where $\mathbf{t}_1$ and $\mathbf{t}_2$ are the tangent unit vectors to diagonals Γ_1 and Γ_2, respectively; $\delta(\circ)$ are Dirac-delta lines with support on the diagonals and $N(\circ)$ are the values of the singular stresses projected on the plane (x, y).

In particular, following [44] and with reference to the diagonal Γ_1, it is possible to calculate the singular stress component $N(\Gamma_1)$ as the jump of the slope of F orthogonally to the singularity line, that is:

$$N(\Gamma_1) = \nabla F(x, y)\big|_{\Gamma_1} \cdot \mathbf{n} \tag{48}$$

where $\mathbf{n}$ is the normal unit vector at Γ_1. The same holds for the diagonal curve Γ_2.

From the projections of the membrane stresses on the horizontal plane, actual membrane stresses can be obtained, both the regular and the singular part, by using (8), i.e., by a projection on the surface of the membrane. the achieved results are summarized in Figure 16 .

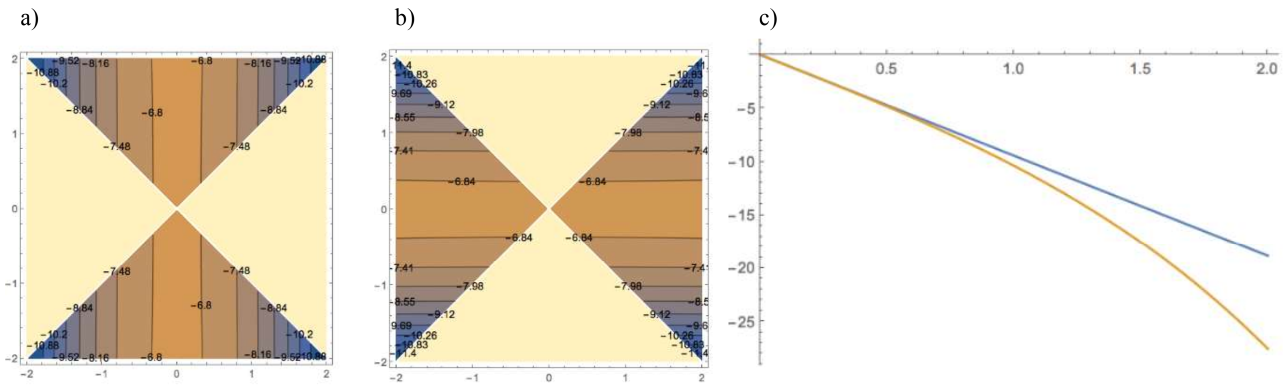

Figure 16. Admissible stress field for the case study cross vault: (a) distribution of N_x [kN/m]; (b) distribution of N_y [kN/m]; (c) projected axial force N [kN] along the diagonals (in blue) and actual axial force along the fold (in orange).

From the mechanical point of view, the statically admissible stress field determined by TSM configure a mechanical behavior of the cross vault as a series of compressed arches parallel to the sides that completely transfer the external load to the folds, which in turn transfer the load towards the supports (Figure 17).

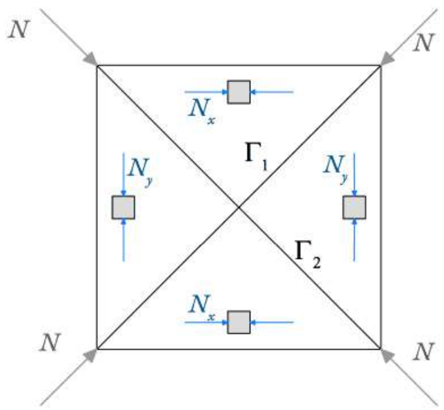

Figure 17. Scheme of the mechanical behavior of the cross vault subject to the self-weight

It is also interesting to note that, differently from the case of a classic masonry arch subject to the self-weight, the thrust in the diagonal arches of the vault is not constant (Figure 16c).

Moreover, from the singular stress component $\mathbf{S}_s$ on the fold (Figure 16c), it is possible to determine the horizontal and vertical the components of the force transmitted to the abutments. After simple calculations, we find $H = 18.05$ kN/m and $V = 18.21$ kN/m . In order to validate this result, it is possible to calculate the resultant of the applied loads by integrating over the domain of the horizontal projection of the vault the assigned load condition; we get:

$$P = \iint_{\Psi} \overline{p}_z \, dA = 74.65 \text{ kN}, \tag{49}$$

for the overall vertical load P. Due to the double symmetry of the problem, the vertical component of the force transmitted to the supports should be equal to $V = P/4 = 18.66$ kN, with an error of 2.41% with respect to the above-reported value determined by TSM.

(ii) Maximum and minimum thrust solutions

By applying TSM with the objective function (27) it is possible to provide an estimation of the maximum and minimum thrust that the cross vault transmits to the supports when it is loaded only with the self-weight (32). The obtained results are shown in Figure 18a-b; in particular, Figure 18a depicts the shape of the maximum thrust equilibrium membrane (in orange), contained between the intrados surface (in light blue) and the extrados surface (in green) of the vault; the same for Figure 18b, now for the case of the minimum thrust equilibrium membrane.

In the same way as in the previous case of the maximum GFS, once determined *(f, F)* the regular membrane stress component $\mathbf{S}_r$ and the singular stress component $\mathbf{S}_s$, concentrated along the two fold lines, can be calculated. To this aim, the partial derivatives of the Airy stress function *F* have to be evaluated, and (47)-(48) have to be employed for evaluating $\mathbf{S}_s$.

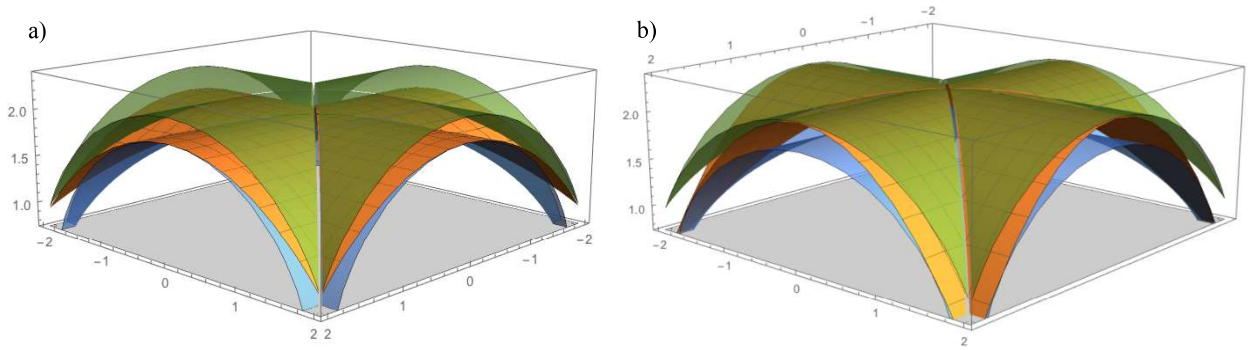

Figure 18. (a) Maximum thrust solution; (b) minimum thrust solution.

Finally, from the singular stress component $\mathbf{S}_s$ on the folds it is possible to determine the horizontal and the vertical components of the forces transmitted to the abutments. In particular, after simple calculations, we get a maximum horizontal thrust $H_{max} = 24.65$ kN and a minimum horizontal thrust $H_{min} = 13.94$ kN. Thus, whatever the admissible equilibrium solution is, the horizontal thrust H at the abutments must be such that:

$$13.94 \text{ kN} \leq H \leq 24.65 \text{ kN}. \tag{50}$$

Recalling (49), we have then obtained that the horizontal thrust H on the abutments is between 18.67% and 33.02% of the resultant P of the applied loads (49). These values are in perfect agreement with the results in [4,26], and [64].

Finally, for the same considerations developed for the case of the barrel vault, the geometry assumed by the equilibrium membrane in the limit conditions of maximum or minimum thrust can provide useful indications on the kinematics of the collapse of the cross vault under the self-weight. In particular, the minimum thrust solution shows tangency zones between the thrust surface and the intrados and the extrados of the vault perfectly corresponding to the hinge zones in the presence of diagonal settlements of the abutments described in [4,64].

For what concerns the computational costs, the analysis of the cross vault has been completed in 51 s by using a common personal computer Intel Core I7-4770 equipped with 16GB of RAM.

6. **Conclusion**

The innovative Thrust Surface Method (TSM) proposed in this paper represents an advanced application of the lower bound theorem of Limit Analysis to masonry vaults of arbitrary shape, aimed at determining the structural safety level of these iconic constructions with reference to general loading conditions.

In the spirit of the lower bound theorem, rather than looking for a generic statically admissible solution, TSM aims at finding of "optimal" solutions, able to fully explore the entire load-bearing capacity spectrum of the vault. To this end, the employ of a convenient numerical procedure together with the formulation of a suitable constrained optimization problem allows us for finding optimal lower bound estimates for:

- the value of the Geometrical Factor of Safety (GFS) of the vault;
- the value of the maximum and minimum thrust that the vault exerts on the abutments;
- the collapse multiplier in a generic live loading process.

The adopted numerical formulation, that can be efficiently coupled with optimization tools, allows for considerably extending the capability and the quality of the obtainable results with respect to other equilibrium approaches in Literature. In particular, vaults of any geometry and under any loading condition (including seismic loads) can be studied by TSM, and the search of optimal lower bound results allows for closely approximate the actual load bearing capacity of the vault. Moreover, TSM does not require assumptions on the load paths or on the topology of the network as in discrete approaches: those assumptions do not allow for exploring the whole set of admissible solutions, and this could affect the quality of results especially for complex geometries and/or load conditions. Finally, in our opinion the special formulation of TSM makes the proposed approach very suitable for practical applications.

It is interesting to point out that from limit solutions obtainable by TSM it is possible to achieve also kinematic information about possible collapse mechanisms of masonry vaults, a topic that, from a literature review, seems do not have enough level of knowledge yet.

From the computational point of view, the analyses reported in *Sect. 5* have been performed with a remarkable speed and efficiency. Indeed, these analyses have been completed in less than a minute by using a common personal computer.

Our innovative approach is in continuity with the classic equilibrium-based methods that have characterized the tradition of analysis and design of masonry structures along centuries, and can be considered as a natural extension to three-dimensional constructions of principles and methods of the thrust line analysis traditionally used for masonry arches. In our opinion, TSM has also the advantage of highlighting the close relationship between shape and structure, a crucial feature of masonry vault and domes, synthetizing one of the highest achievements of the traditional construction techniques.

The effectiveness of the method, in light of different case studies, was proved by the comparison of TSM results with well-established analytical, numerical and experimental results in the literature. For the sake of this comparison, in the analyzed case studies only the self-weight of the vault has been considered as the loading condition, similarly to the reference cases taken from the literature.

More general load conditions (for example, the study of the role of the infill like in [65], or the assessment of the load bearing capacity of masonry vaults subject to horizontal forces) will be analyzed in forthcoming papers. Moreover, in the next future TSM will be applied to some real-life masonry vaults characterized by more complex loads and boundary conditions. In addition, the influence of structural pathologies (as pre-existing crack patterns) on the load-bearing capacity of the vault will also be evaluated. Finally, further developments will extend the capabilities of TSM to the reinforcement design, by using suitable spatial extensions of approaches proposed in the literature mainly for masonry arches [66], in which the additional tensile strength offered by reinforcements is represented through a virtual geometric extension of the spatial admissibility domain of the thrust surface.

Appendix A – An analytical Validation of TSM results

For validating TSM, with reference to results in *Sect. 5.2* concerning the case of the barrel vault in minimum thrust condition, it is possible to observe that the value of the minimum thrust can be evaluated analytically by studying the equilibrium of a portion of the cross section of the vault between two consecutive hinges (see Figure 11). With reference to Figure 19 and following the approach in [4,59], the minimum thrust can be determined as:

$$H_{\min} = \gamma\beta \frac{\left(r_{ext}^2 - r_{\text{int}}^2\right)}{\left(r_{ext} - r_{\text{int}} \cos 2\beta\right)} \left[r_{\text{int}} \cos\theta - \frac{2\left(r_{ext}^3 - r_{\text{int}}^3\right)}{3\left(r_{ext}^2 - r_{\text{int}}^2\right)} \sin\beta \right], \tag{A.52}$$

where θ assigns the position of the inner hinge and $2\beta = \frac{\pi}{2} - \theta$ is the angle of embrace between two consecutive hinges.

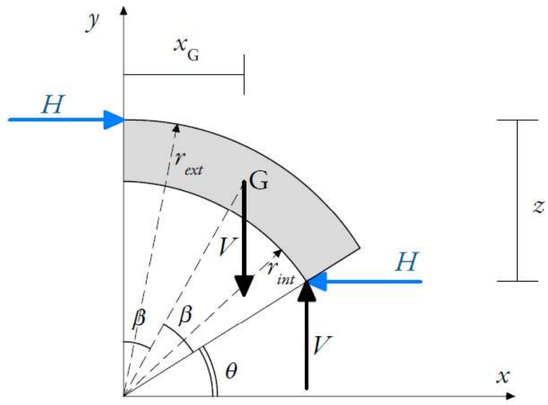

Figure 19. Scheme for the analytical expression of the minimum thrust for an arch having a segmental profile [4]

For the vault under examination (A.52) provides the value H_{min} = 4.80 kN/m. The minimum thrust estimated by TSM H_{min} = 4.99 kN/m is then in very good agreement with the analytical result: the difference is limited to 3.82%, absolutely negligible for practical applications.

References

[1] Roca P, Cervera M, Gariup G, Pela' L. Structural analysis of masonry historical constructions. Classical and advanced approaches. Arch Comput Methods Eng 2010. doi:10.1007/s11831-010-9046-1.

[2] Tralli A, Alessandri C, Milani G. Computational Methods for Masonry Vaults: A Review of Recent Results. Open Civ Eng J 2014;8:272–87. doi:10.2174/1874149501408010272.

[3] Huerta S. Mechanics of masonry vaults: The equilibrium approach. 3rd Int. Semin. Hist. Constr. Guimarães, Port., 2001.

[4] Como M. Statics of Historic Masonry Constructions. Third Edit. Springer; 2016.

[5] Cavalagli N, Gusella V, Severini L. Lateral loads carrying capacity and minimum thickness of circular and pointed masonry arches. Int J Mech Sci 2016. doi:10.1016/j.ijmecsci.2016.07.015.

[6] Milani G, Valente M. Comparative pushover and limit analyses on seven masonry churches damaged

by the 2012 Emilia-Romagna (Italy) seismic events: Possibilities of non-linear finite elements compared with pre-assigned failure mechanisms. Eng Fail Anal 2015. doi:10.1016/j.engfailanal.2014.09.016.

[7] Portioli F, Casapulla C, Gilbert M, Cascini L. Limit analysis of 3D masonry block structures with non-associative frictional joints using cone programming. Comput Struct 2014;143. doi:10.1016/j.compstruc.2014.07.010.

[8] Alexakis H, Makris N. Hinging Mechanisms of Masonry Single-Nave Barrel Vaults Subjected to Lateral and Gravity Loads. J Struct Eng 2017;143:04017026. doi:10.1061/(ASCE)ST.1943-541X.0001762.

[9] Di Pasquale S. New trends in the analysis of masonry structures. Meccanica 1992;27:173–84. doi:10.1007/BF00430043.

[10] Del Piero G. Constitutive equation and compatibility of the external loads for linear elastic masonry-like materials. Meccanica 1989;24:150–62. doi:10.1007/BF01559418.

[11] Angelillo M. Constitutive relations for no-tension materials. Meccanica 1993;28:195–202. doi:10.1007/BF00989121.

[12] Giaquinta M, Giusti E. Researches on the equilibrium of masonry structures. Arch Ration Mech Anal 1985. doi:10.1007/BF00250872.

[13] Sacco E. Modellazione e calcolo di strutture in materiale non resistente a trazione. Rend Lincei - Mat e Appl 1990;1:235–58.

[14] Del Piero G. Limit analysis and no-tension materials. Int J Plast 1998;14:259–71. doi:10.1016/S0749-6419(97)00055-7.

[15] Heyman J. The stone skeleton. Int J Solids Struct 1966;2:249–79. doi:10.1016/0020-7683(66)90018-7.

[16] Heyman J. The stone skeleton: Structural engineering of masonry architecture. UK: Cambridge University Press; 1995. doi:10.1017/CBO9781107050310.

[17] Wolfe WS. Graphical analysis: a handbook on graphic statics. New York: McGraw Hill; 1921.

[18] Bagi K. When Heyman's Safe Theorem of rigid block systems fails: Non-Heymanian collapse modes of masonry structures. Int J Solids Struct 2014. doi:10.1016/j.ijsolstr.2014.03.041.

[19] Beatini V, Royer-Carfagni G, Tasora A. The role of frictional contact of constituent blocks on the stability of masonry domes. Proc R Soc A Math Phys Eng Sci 2018. doi:10.1098/rspa.2017.0740.

[20] Beatini V, Royer-Carfagni G, Tasora A. Modeling the shear failure of segmental arches. Int J Solids Struct 2019. doi:10.1016/j.ijsolstr.2018.08.023.

[21] Milani E, Milani G, Tralli A. Limit analysis of masonry vaults by means of curved shell finite elements and homogenization. Int J Solids Struct 2008;45:5258–88. doi:10.1016/j.ijsolstr.2008.05.019.

[22] Chiozzi A, Milani G, Tralli A. Fast Kinematic Limit Analysis of FRP-Reinforced Masonry Vaults. I: General Genetic Algorithm–NURBS–Based Formulation. J Eng Mech 2017. doi:10.1061/(asce)em.1943-7889.0001267.

[23] Chiozzi A, Milani G, Tralli A. Fast Kinematic Limit Analysis of FRP-Reinforced Masonry Vaults. II: Numerical Simulations. J Eng Mech 2017. doi:10.1061/(asce)em.1943-7889.0001268.

[24] O'Dwyer D. Funicular analysis of masonry vaults. Comput Struct 1999. doi:10.1016/S0045-7949(98)00279-X.

[25] Block P, Ochsendorf J. Thrust network analysis: A new methodology for three-dimensional equilibrium. J. Int. Assoc. Shell Spat. Struct., 2007.

[26] Block P. Thrust network analysis: exploring three-dimensional equilibrium. MIT, 2009.

[27] Foti P, Fraddosio A, Lepore N, Piccioni MD. On the mechanics of corbelled domes: new analytical and computational approaches. Res Eng Struct Mater 2017;3:210–26. doi:10.17515/resm2016.71st0725.

[28] Foti P, Fraddosio A, Lepore N, Mario Daniele Piccioni. Three-dimensional lower-bound analysis of masonry structures. Struct. Archit. Beyond their Limits, CRC Press; 2016, p. 558–66.

[29] Marmo F, Rosati L. Reformulation and extension of the thrust network analysis. Comput Struct 2017. doi:10.1016/j.compstruc.2016.11.016.

[30] Marmo F, Masi D, Rosati L. Thrust network analysis of masonry helical staircases. Int J Archit Herit 2018;12:828–48. doi:10.1080/15583058.2017.1419313.

[31] Block P, Lachauer L. Three-dimensional (3D) equilibrium analysis of gothic masonry vaults. Int J Archit Herit 2014;8:312–35. doi:10.1080/15583058.2013.826301.

[32] Baratta A, Corbi O. On the statics of No-Tension masonry-like vaults and shells: Solution domains, operative treatment and numerical validation. Ann Solid Struct Mech 2011;2:107–22. doi:10.1007/s12356-011-0022-8.

[33] Angelillo M, Fortunato A. Equilibrium of masonry vaults. Lect Notes Appl Comput Mech 2004;14:105–11. doi:10.1007/978-3-540-45287-4.

[34] Barsotti R, Bennati S, Stagnari R. Analytical determination of statically admissible thrust surfaces for the limit analysis of masonry vaults and domes. AIMETA 2017 - Proc 23rd Conf Ital Assoc Theor Appl Mech 2017;2:4–7. doi:10.1037/0735-7028.36.3.330.

[35] Lucchesi M, Šilhavý M, Zani N. Singular equilibrated stress fields for no-tension panels. In: Frédmond M, Maceri F, editors. Lect. notes Appl. Comput. Mech., vol. 23, Berlin: Springer; 2005, p. 255–65.

[36] Lucchesi M, Šilhavý M, Zani N. A new class of equilibrated stress fields for no-tension bodies. J Mech Mater Struct 2006;1:503–39.

[37] Lucchesi M, Šilhavý M, Zani N. On the balance equation for stresses concentrated on curves. J Elast 2008;90:209–23. doi:10.1007/s10659-007-9139-8.

[38] Angelillo M, Babilio E, Fortunato A. Singular stress fields for masonry-like vaults. Contin Mech Thermodyn 2013;25:423–41. doi:10.1007/s00161-012-0270-9.

[39] Contestabile M, Babilio E, Fortunato A, Guerriero L, Lippiello M, Pasquino M, et al. Static Analysis of Cross Vaults: The Case of the Cathedral of Casertavecchia. Open Constr Build Technol J 2016;10:329–45. doi:10.2174/1874836801610010329.

[40] Gesualdo A, Cennamo C, Fortunato A, Frunzio G, Monaco M, Angelillo M. Equilibrium formulation of masonry helical stairs. Meccanica 2017;52:1963–74. doi:10.1007/s11012-016-0533-9.

[41] Flügge W. Stresses in Shells. Berlin, Heidelberg: Springer Berlin Heidelberg; 1973. doi:10.1007/978-3-642-88291-3.

[42] Fosdick R, Foti P, Fraddosio A, Marzano S, Piccioni MD. A lower bound estimate of the critical load in bifurcation analysis for incompressible elastic solids. Math Mech Solids 2015;20:53–79. doi:10.1177/1081286514543599.

[43] de Felice G, De Santis S, Lourenço PB, Mendes N. Methods and Challenges for the Seismic Assessment of Historic Masonry Structures. Int J Archit Herit 2017. doi:10.1080/15583058.2016.1238976.

[44] Angelillo M. Mechanics of Masonry Structures. Springer-Verlag Wien; 2014. doi:10.1007/978-3-7091-1774-3.

[45] Fortunato A, Babilio E, Lippiello M, Gesualdo A, Angelillo M. Limit Analysis for Unilateral Masonry-like Structures. Open Constr Build Technol J 2016;10:346–62. doi:10.2174/1874836801610010346.

[46] Fraddosio A, Lepore N, Piccioni MD. Lower Bound Limit Analysis of Masonry Vaults Under General Load Conditions. RILEM Bookseries, 2019. doi:10.1007/978-3-319-99441-3_118.

[47] Lepore N. Le volte in muratura: forma e struttura, equilibrio e analisi limite. PhD dissertation, Università degli Studi RomaTRE, 2018.

[48] Pratt V. Direct least-squares fitting of algebraic surfaces. ACM SIGGRAPH Comput Graph

1987;21:145–52. doi:10.1145/37402.37420.

[49] Goshtasby A, O'Neill WD. Surface fitting to scattered data by a sum of Gaussians. Comput Aided Geom Des 1993;10:143–56. doi:10.1016/0167-8396(93)90017-W.

[50] Alexa M, Behr J, Cohen-Or D, Fleishman S, Levin D, Silva CT. Computing and rendering point set surfaces. IEEE Trans Vis Comput Graph 2003. doi:10.1109/TVCG.2003.1175093.

[51] Miki M, Igarashi T, Block P. Parametric self-supporting surfaces via direct computation of airy stress functions. ACM Trans Graph 2015;34:89:1-89:12. doi:10.1145/2766888.

[52] Flügge W, Geyming FT. A general theory of deformations of membrane shells. IABSE Pubblication 1957:23–46. doi:10.5169/seals-15752.

[53] Save M, Prager W. Structural Optimization, Vol.2: Mathematical Programming. 1st ed. New York: Plenum Press; 1990.

[54] Michiels T, Adriaenssens S. Form-finding algorithm for masonry arches subjected to in-plane earthquake loading. Comput Struct 2018. doi:10.1016/j.compstruc.2017.10.001.

[55] Nocedal J, Wright SJ. Numerical Optimization. Springer New York; 2006. doi:10.1007/978-0-387-40065-5.

[56] Storn R, Price K. Differential Evolution - A Simple and Efficient Heuristic for Global Optimization over Continuous Spaces. J Glob Optim 1997;11:341–59. doi:10.1023/A:1008202821328.

[57] Fraternali F. A thrust network approach to the equilibrium problem of unreinforced masonry vaults via polyhedral stress functions. Mech Res Commun 2010. doi:10.1016/j.mechrescom.2009.12.010.

[58] Heyman J. The safety of masonry arches. Int J Mech Soc 1969. doi:10.1016/0020-7403(69)90070-8.

[59] Ochsendorf J. Collapse of masonry structures. Cambridge University, 2002.

[60] Ricci E, Fraddosio A, Piccioni MD, Sacco E. Numerical methods for the lower bound limit analysis of masonry arches. AIMETA 2017 - Proc. 23rd Conf. Ital. Assoc. Theor. Appl. Mech., vol. 2, 2017.

[61] Ricci E, Fraddosio A, Piccioni MD, Sacco E. A new numerical approach for determining optimal thrust curves of masonry arches. Eur J Mech A/Solids 2019. doi:10.1016/j.euromechsol.2019.02.003.

[62] Shapiro EE. Collapse mechanisms of small-scale unreinforced masonry vaults. Master Thesis, Massachusetts Institute of Technology, 2012.

[63] Ochsendorf J. The masonry arch on spreading supports. Struct Eng 2006;84:29–35.

[64] Intrigila C, Nodargi NA, Bisegna P. Square Cross Vaults on Spreading Supports. In: Aguilar R, Torrealva D, Moreira S, Pando MA, Ramos LF, editors. Struct. Anal. Hist. Constr., vol. 18, Springer International Publishing; 2019, p. 1045–53. doi:10.1007/978-3-319-99441-3_113.

[65] Fraddosio A, Lepore N, Piccioni MD. Further refinement of the Corbelling Theory for the equilibrium analysis of corbelled domes. Curved Layer Struct 2019;6:29–39. doi:10.1515/cls-2019-0003.

[66] Ramaglia G, Lignola GP, Prota A. Collapse analysis of slender masonry barrel vaults. Eng Struct 2016;117:86–100. doi:10.1016/j.engstruct.2016.03.016.